

Exploring Relativistic World of Electromagnetism on Computer

Daiju Nakayama,^{*} Kin-ya Oda,[†] and Koichiro Yasuda[‡]

^{*} *e-Seikatsu Co., Ltd., 5-2-32, Tokyo 106-0047, Japan*

[†] *Department of Information and Mathematical Sciences,
Tokyo Woman's Christian University, Tokyo 167-8585, Japan*

[‡] *Department of Physics and Astronomy, University of California, Los Angeles,
California 90095-1547, USA*

August 13, 2024

Abstract

It is the theoretical structure of electromagnetism that led Einstein to special relativity. To foster an intuitive understanding of relativity's core idea, it is valuable to create a fully special relativistic computer simulation incorporating electromagnetic dynamics. In this paper, we provide a basic formulation for such an implementation. Specifically, the player observes the world via their past light cone and experiences the Lorentz force generated by the electromagnetic field at their spacetime location. The electromagnetic field at any given spacetime point is determined by the sublight-speed motion of individual point charges on the past light cone of that spacetime point.

^{*}E-mail: 42.daiju@gmail.com

[†]E-mail: odakin@lab.twcu.ac.jp

[‡]E-mail: yasuda@physics.ucla.edu

Contents

1	Introduction	3
2	Special relativity on computer	4
2.1	Spacetime coordinates	4
2.2	Lorentz transformation	6
2.3	Light cone	6
2.4	Proper time and covariant velocity	8
2.5	Lorentz transformation to rest frame	10
2.6	Covariant acceleration	10
2.7	Past light cone	11
2.8	Worldlines and their intersections with player's PLC	11
2.9	Drawing world	13
2.10	Special relativistic equation of motion	13
2.11	Player's time evolution	13
2.12	Time evolution of others	14
3	Relativistic electromagnetism	15
3.1	Equation of motion	15
3.2	Relativistic Maxwell's equation	16
3.3	Relativistic Maxwell's equations	18
3.4	General solution to relativistic Maxwell's equation	19
4	Covariant formalism for field strength from point charges	20
4.1	Continuous worldlines and covariant current density	20
4.2	Master equation for gauge field	21
4.3	Field strength	24
4.4	Electromagnetic field	26
4.5	Comparison with literature	27
4.6	Various limits	28
5	Overview of concrete implementation	29
5.1	Speed of Light	29
5.2	Arrow	30
5.3	Preset	32
5.4	Grid	32
5.5	Controls	32
6	Conclusion	33

1 Introduction

Special relativity, along with quantum mechanics, forms the basis of quantum field theory, which serves as the fundamental language of the Standard Model of particle physics [1]. In a classical (non-quantum) world, special relativity is a theory that describes the motion of objects within the four-dimensional Minkowski spacetime and the outcomes resulting from Lorentz transformations that leave all the speeds of light unchanged. The relativistic effects become increasingly noticeable as an object’s speed approaches the speed of light. Unlike quantum mechanical effects, these relativistic effects can be perceived by everyday human perception, namely, through our sense of sight. Visualization of these effects via three-dimensional (3D) simulations greatly helps comprehension of the fundamental idea of relativity.

Ref. [2] provides an accurate implementation of special relativity in computer games, incorporating elements such as time dilation, Lorentz contraction, causality, and the Doppler effect, while also dealing with challenges related to projecting distant scenes onto skydome and approximating polygon-based rigid bodies; see also its Introduction for earlier attempts. Within this framework, each object retains data regarding its worldline. In a departure from conventional, non-relativistic game mechanics—in which a player renders objects on an equal-time hyperplane—the world perceived by the player is its past light cone (PLC). Indeed, any observer at any spacetime point observes other objects at the points of intersection with the observer’s PLC, a structure that maintains system-wide causality. When the observer sees the world through its PLC, a Lorentz transformation can be applied to these intersection points, enabling the realization of Lorentz contraction in the observer’s instantaneous rest frame, as well as the time dilation. Importantly, this PLC framework demonstrates both Lorentz contraction and the often-overlooked Lorentz *stretching*.

Einstein’s conceptualization of special relativity was catalyzed by the understanding that electric and magnetic fields are mixed when inertial frames are transformed among each other [3]. Given this, developing a computer simulation that embodies a world governed by electromagnetic dynamics can provide a more profound and intuitive understanding of relativity. Nevertheless, current research has limited its focus on visualizing relativistic motions without electromagnetism.

In this study, we fill the gap by introducing a basic formulation to incorporate electromagnetism into the relativistic algorithm proposed in Ref. [2]. Our approach entails three primary steps: First, we visualize the intermingling of electric and magnetic fields on each spacetime point of the player’s PLC, resulting from changes in the player’s inertial systems. That is, by applying a Lorentz transformation, each electromagnetic field tensor at the point of intersection with the player’s PLC is converted into that in the player’s rest system, thus yielding the visual representation of the intermingling of the electromagnetic field. Second, every charged particle—including the player—can experience the Lorentz force due to the electromagnetic field at its specific spacetime point \vec{x} (see below for notation). Lastly, the electromagnetic field at \vec{x} is determined by the spacetime motions (both positions and velocities) of charged particles on the PLC of \vec{x} . This approach ensures a fully relativistic account of the interaction between the electromagnetic field and charged particles. In particular, we formulate everything in a manifestly Lorentz-covariant manner.

As a concrete example, we introduce a novel simulator and visualize the observer-dependent relativistic electromagnetic field. This innovative simulation is expected to aid students in visually grasping relativistic effects, thereby enhancing their understanding when introduced

to relativity theory in lectures.

This paper is organized as follows:

Here, we do not omit details that, while potentially elementary for physics experts, are important for ensuring accessibility to a broader audience.

2 Special relativity on computer

In this section, we review the formalism of Ref. [2] to spell out our notation. Here, we do not omit some details that, while potentially elementary for physics or mathematics experts, are important for ensuring accessibility to a broader audience.

Special Relativity, formulated within the context of flat spacetime, is founded on the following two primary postulates:

- I. The constancy of the speed of light in vacuum.
- II. Lorentz invariance, implying the laws of physics are the same for all inertial observers.

Additionally, this paper considers the application of the equivalence principle in a special relativistic framework.

- III. The equivalence principle, adapted for specific contexts within Special Relativity.

The principle I is central to the discussions in Sections 2.1 and 2.2. The principle II is applied and elaborated upon in Sections 2.2–2.8. The adapted equivalence principle III finds its application in Section 2.10, with the aid of Sec. 2.6.

2.1 Spacetime coordinates

We first prepare a Cartesian coordinate system for a reference frame, which we call the *world frame* hereafter:

$$\vec{x} = (x^0, \mathbf{x}) = (x^0, x^1, x^2, x^3), \quad (1)$$

where

$$x^0 := ct \quad (2)$$

denotes the time t multiplied by the (constant) speed of light c and $\mathbf{x} = (x^1, x^2, x^3)$ is the spatial coordinates, which are more frequently (but not in this paper) written as (x, y, z) . Hereafter, we call x^0 , having the dimension of length, the *time length*. If one does not intend to change the speed of light depending on the game/simulation settings, one may take the *natural units*

$$c = 1. \quad (3)$$

Throughout this paper, we keep the non-natural units for the possible reader's ease.

We also employ the matrix notation

$$\vec{x} = \begin{bmatrix} x^0 \\ \mathbf{x} \end{bmatrix} = \begin{bmatrix} x^0 \\ x^1 \\ x^2 \\ x^3 \end{bmatrix}, \quad \vec{x}^t = [x^0 \quad \mathbf{x}^t] = [x^0 \quad x^1 \quad x^2 \quad x^3], \quad (4)$$

where the superscript “t” denotes the transpose.

In the actual implementation in Sec. 5, the spatial and time-length coordinates are indexed as

$$\begin{bmatrix} \mathbf{x} \\ \mathbf{y} \\ \mathbf{z} \\ \mathbf{w} \end{bmatrix} = \begin{bmatrix} \mathbf{x}[0] \\ \mathbf{x}[1] \\ \mathbf{x}[2] \\ \mathbf{x}[3] \end{bmatrix} := \begin{bmatrix} x^1 \\ x^2 \\ x^3 \\ x^0 \end{bmatrix}. \quad (5)$$

The authors are sorry for the confusing notation but this is how the physics and information-technology communities translate.

For spatial vectors $\mathbf{x} = (x^1, x^2, x^3)$ and $\mathbf{y} = (y^1, y^2, y^3)$, we write their inner product

$$\mathbf{x} \cdot \mathbf{y} := \sum_{i=1}^3 x^i y^i = [x^1 \quad x^2 \quad x^3] \begin{bmatrix} y^1 \\ y^2 \\ y^3 \end{bmatrix} = \mathbf{x}^t \mathbf{y}, \quad (6)$$

$$\mathbf{x}^2 := \mathbf{x} \cdot \mathbf{x} = (x^1)^2 + (x^2)^2 + (x^3)^2 = \sum_{i=1}^3 (x^i)^2, \quad (7)$$

$$|\mathbf{x}| := \sqrt{\mathbf{x}^2} = \sqrt{(x^1)^2 + (x^2)^2 + (x^3)^2} = \sqrt{\sum_{i=1}^3 (x^i)^2}. \quad (8)$$

Throughout this paper, the roman and greek letters i, j, \dots and μ, ν, \dots run for 1, 2, 3 and 0, \dots , 3, respectively. A hat symbol denotes a unit vector:

$$\hat{\mathbf{x}} := \frac{\mathbf{x}}{|\mathbf{x}|}. \quad (9)$$

For later use, we define a matrix called *metric*:

$$\eta = [\eta_{\mu\nu}]_{\mu, \nu=0, \dots, 3} = \begin{bmatrix} \eta_{00} & \eta_{01} & \eta_{02} & \eta_{03} \\ \eta_{10} & \eta_{11} & \eta_{12} & \eta_{13} \\ \eta_{20} & \eta_{21} & \eta_{22} & \eta_{23} \\ \eta_{30} & \eta_{31} & \eta_{32} & \eta_{33} \end{bmatrix} := \begin{bmatrix} -1 & 0 & 0 & 0 \\ 0 & 1 & 0 & 0 \\ 0 & 0 & 1 & 0 \\ 0 & 0 & 0 & 1 \end{bmatrix}. \quad (10)$$

Here and hereafter, we use the sans-serif italic font to denote matrices. Since $\eta^2 = I$, where I denotes an identity matrix in the corresponding number of dimensions (= 4 in the current case), the inverse of η becomes identical to itself: $\eta^{-1} = \eta$, where

$$\eta^{-1} = [\eta^{\mu\nu}]_{\mu, \nu=0, \dots, 3} = \begin{bmatrix} \eta^{00} & \eta^{01} & \eta^{02} & \eta^{03} \\ \eta^{10} & \eta^{11} & \eta^{12} & \eta^{13} \\ \eta^{20} & \eta^{21} & \eta^{22} & \eta^{23} \\ \eta^{30} & \eta^{31} & \eta^{32} & \eta^{33} \end{bmatrix} = \begin{bmatrix} -1 & 0 & 0 & 0 \\ 0 & 1 & 0 & 0 \\ 0 & 0 & 1 & 0 \\ 0 & 0 & 0 & 1 \end{bmatrix}. \quad (11)$$

Using η , we define the Lorentzian inner product and the Lorentzian (squared-)norm:

$$\begin{aligned} (\vec{x}, \vec{y}) &:= \vec{x}^t \eta \vec{y} = [x^0 \quad x^1 \quad x^2 \quad x^3] \begin{bmatrix} -1 & 0 & 0 & 0 \\ 0 & 1 & 0 & 0 \\ 0 & 0 & 1 & 0 \\ 0 & 0 & 0 & 1 \end{bmatrix} \begin{bmatrix} y^0 \\ y^1 \\ y^2 \\ y^3 \end{bmatrix} \\ &= -x^0 y^0 + \mathbf{x} \cdot \mathbf{y} = -x^0 y^0 + x^1 y^1 + x^2 y^2 + x^3 y^3, \end{aligned} \quad (12)$$

$$(\vec{x})^2 := (\vec{x}, \vec{x}) = -(x^0)^2 + \mathbf{x}^2 = -(x^0)^2 + (x^1)^2 + (x^2)^2 + (x^3)^2. \quad (13)$$

We might sometimes write

$$\vec{x} \cdot \vec{y} := (\vec{x}, \vec{y}), \quad \vec{x}^2 := (\vec{x})^2. \quad (14)$$

2.2 Lorentz transformation

Spetial relativity postulates the light-speed invariance. The coordinates $\mathbf{x} = (x^1, x^2, x^3)$ of a spherical light wave originating from $\mathbf{x} = 0$ at the time length $x^0 = 0$ are prescribed by the following constraint at a time length x^0 :

$$\mathbf{x}^2 = (x^0)^2. \quad (15)$$

This condition for the spherical light wave can be written as

$$(\vec{x})^2 = 0. \quad (16)$$

In the spirit of the light-speed invariance, a linear spacetime-coordinate transformation (represented by a matrix) Λ ,

$$\vec{x} \rightarrow \vec{x}' = \Lambda \vec{x}, \quad \begin{bmatrix} x^0 \\ x^1 \\ x^2 \\ x^3 \end{bmatrix} \rightarrow \begin{bmatrix} x'^0 \\ x'^1 \\ x'^2 \\ x'^3 \end{bmatrix} = \begin{bmatrix} \Lambda^0_0 & \Lambda^0_1 & \Lambda^0_2 & \Lambda^0_3 \\ \Lambda^1_0 & \Lambda^1_1 & \Lambda^1_2 & \Lambda^1_3 \\ \Lambda^2_0 & \Lambda^2_1 & \Lambda^2_2 & \Lambda^2_3 \\ \Lambda^3_0 & \Lambda^3_1 & \Lambda^3_2 & \Lambda^3_3 \end{bmatrix} \begin{bmatrix} x^0 \\ x^1 \\ x^2 \\ x^3 \end{bmatrix}, \quad (17)$$

is called the *Lorentz transformation* when it leaves the left-hand side of Eq. (16) invariant: For all \vec{x} ,

$$(\vec{x}')^2 = (\vec{x})^2 \iff (\Lambda \vec{x})^t \eta (\Lambda \vec{x}) = \vec{x}^t \eta \vec{x} \iff \vec{x}^t (\Lambda^t \eta \Lambda) \vec{x} = \vec{x}^t \eta \vec{x}. \quad (18)$$

That is, a transformation (represented by) Λ is called the Lorentz transformation when and only when¹

$$\Lambda^t \eta \Lambda = \eta. \quad (19)$$

This can be equivalently written as

$$\Lambda^{-1} = \eta \Lambda^t \eta. \quad (20)$$

When a “spacetime vector” $\vec{V} = (V^0, V^1, V^2, V^3)$ transforms the same as the coordinates \vec{x} under the Lorentz transformations (17), namely $\vec{V} \rightarrow \vec{V}' = \Lambda \vec{V}$, we call \vec{V} a *covariant* vector.² Special relativity is a theory that describes everything in terms of covariant and invariant quantities.

2.3 Light cone

The above argument sets the spacetime origin as the reference point. Now we generalize it. Given a reference point \vec{x}_r and another arbitrary point \vec{x} , let us consider the following

¹ This relation results in $\det \Lambda = \pm 1$ and $|\Lambda^0_0| \geq 1$. Hereafter, when we say Lorentz transformation, it denotes the proper ($\det \Lambda = 1$) orthochronous ($\Lambda^0_0 \geq 1$) Lorentz transformation, barring the parity transformation (or space inversion) $P := \text{diag}(1, -1, -1, -1)$ and the time reversal $T := \text{diag}(-1, 1, 1, 1)$, where “diag” denotes the diagonal matrix.

²In this paper, we call both the contravariant and covariant vectors the covariant vectors in the spirit that both are Lorentz covariant.

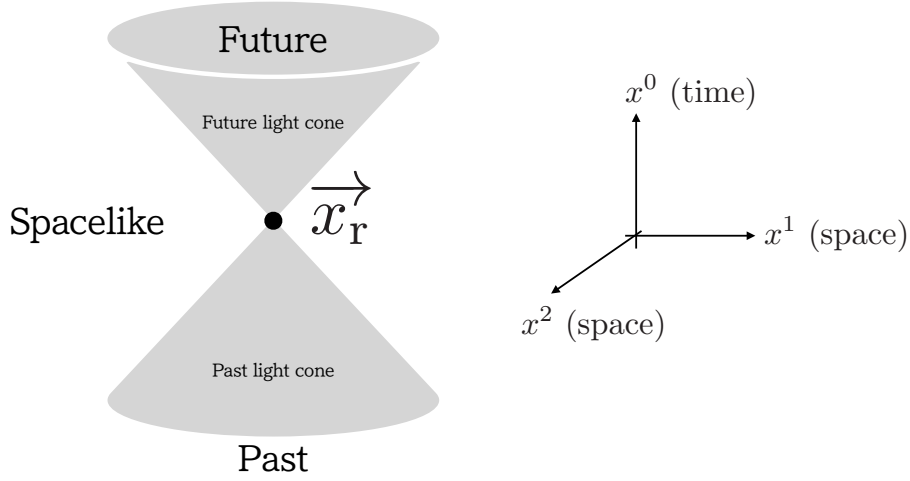


Figure 1: Schematic figure (in two spatial dimensions) for the past, spacelike, and future regions of \vec{x}_r , as well as its future and past light cones.

Lorentz *invariant*:

$$(\vec{x} - \vec{x}_r)^2 = -(x^0 - x_r^0)^2 + (\mathbf{x} - \mathbf{x}_r)^2. \quad (21)$$

With it, we may divide the whole spacetime into three regions (see Fig. 1):

- \vec{x} belongs to the *past* region of \vec{x}_r if the separation is *timelike* $(\vec{x} - \vec{x}_r)^2 < 0$ and if $x^0 < x_r^0$.
- \vec{x} belongs to the *spacelike* region of \vec{x}_r if the separation is *spacelike* $(\vec{x} - \vec{x}_r)^2 > 0$.
- \vec{x} belongs to the *future* region of \vec{x}_r if the separation is *timelike* $(\vec{x} - \vec{x}_r)^2 < 0$ and if $x^0 > x_r^0$.

These three regions are separated by the *light cones*:

- \vec{x} belongs to the *past light cone* (PLC) of \vec{x}_r if the separation is *lightlike* $(\vec{x} - \vec{x}_r)^2 = 0$ and if $x^0 < x_r^0$.
- \vec{x} belongs to the *future light cone* of \vec{x}_r if the separation is *lightlike* $(\vec{x} - \vec{x}_r)^2 = 0$ and if $x^0 > x_r^0$.

We emphasize that the three regions and the light cones are defined independently of the chosen coordinate system.³

³ The order of times is Lorentz invariant when the separation is either timelike or lightlike; see also footnote 1.

2.4 Proper time and covariant velocity

Let us consider objects O_1, O_2, \dots . We write the O_n 's spacetime position \vec{x}_n . In the next iteration of the computer program, it moves to \vec{x}_n' .⁴ From the displacement vector

$$\vec{\Delta x}_n := \vec{x}_n' - \vec{x}_n, \quad \begin{bmatrix} \Delta x_n^0 \\ \Delta \mathbf{x}_n \end{bmatrix} = \begin{bmatrix} x_n'^0 - x_n^0 \\ \mathbf{x}_n' - \mathbf{x}_n \end{bmatrix}, \quad (22)$$

we may define a Lorentz invariant: $\left(\vec{\Delta x}_n\right)^2 = -(\Delta x_n^0)^2 + (\Delta \mathbf{x}_n)^2$. A particle is called *massive*, *massless*, and *tachyon* when it moves with this Lorentz-invariant quantity being always negative, zero, and positive, respectively:

$$\left(\vec{\Delta x}_n\right)^2 \begin{cases} < 0 & \text{massive (moving timelike),} \\ = 0 & \text{massless (moving lightlike),} \\ > 0 & \text{tachyon (moving spacelike).} \end{cases} \quad (23)$$

The light is massless. Hereafter, we assume all the objects (other than light rays) are massive unless otherwise stated. We also assume that an object moves forward in the future direction: $\Delta x_n^0 > 0$.⁵

Note that by the definition of massiveness,

$$\left(\vec{\Delta x}_n\right)^2 < 0 \iff (\Delta \mathbf{x}_n)^2 < (\Delta x_n^0)^2, \quad (24)$$

the (non-covariant) velocity of the massive particle⁶

$$\mathbf{v}_n := c \frac{d\mathbf{x}_n}{dx_n^0} = \lim_{\Delta x_n^0 \rightarrow 0} c \frac{\Delta \mathbf{x}_n}{\Delta x_n^0} \quad (25)$$

always satisfies

$$|\mathbf{v}_n| < c. \quad (26)$$

That is, all the massive objects move slower than the speed of light.

For each iteration, we define what we call a *proper time distance* for O_n by

$$\Delta s_n := \sqrt{-\left(\vec{\Delta x}_n\right)^2} = \Delta x_n^0 \sqrt{1 - \left(\frac{\Delta \mathbf{x}_n}{\Delta x_n^0}\right)^2}. \quad (27)$$

By adding the proper time distance of all the iterations (up to the spacetime point of interest), we obtain what we call the *proper time length* s_n that parametrizes each world line of O_n ; it becomes the same as the *proper time* $\tau_n := s_n/c$ in natural units $c = 1$.⁷

⁴It should be understood that the prime symbol here, “’”, has nothing to do with the Lorentz transformation (17).

⁵The order of time is well-defined both for massive and massless particles that move into the future and the future-light cone, respectively; see footnote 3. We also note that there is no need to consider an object moving backward in time because, in quantum field theory, a particle moving backward in time is equivalent to an anti-particle moving forward in time, and vice versa.

⁶The expression $\mathbf{v}_n = \frac{d\mathbf{x}_n}{dt}$ in the world frame might be more familiar for some readers; recall Eq. (2).

⁷As we are in the non-natural units, we unconventionally call the proper time (multiplied by c) the proper time length.

In the limit of infinitesimal iterations, the proper time length s_n becomes a continuous parameter. It is important that the proper time length can parametrize the O_n 's *worldline* \mathcal{W}_n in a *Lorentz-invariant* fashion, where \mathcal{W}_n is the trajectory of O_n in the spacetime:

$$\mathcal{W}_n := \{ \vec{x}_n(s_n) \mid s_n^{\text{start}} \leq s_n \leq s_n^{\text{cease}} \}, \quad (28)$$

with s_n^{start} and s_n^{cease} being the proper time lengths at which O_n starts and ceases to exist, respectively.

In the limit of infinitesimal lapse of the proper time length $\Delta s_n \rightarrow 0$, we define the dimensionless *covariant velocity*:

$$\vec{u}_n := \lim_{\Delta s_n \rightarrow 0} \frac{\Delta \vec{x}_n}{\Delta s_n} = \frac{d\vec{x}_n}{ds_n}, \quad (29)$$

where the particle position (on its worldline) is regarded as a function of its proper time length: $\vec{x}_n(s_n)$. Hereafter, when we simply write *velocity*, it denotes the dimensionless covariant velocity, and we always call \mathbf{v}_n the non-covariant velocity.

By definition (27), we see that

$$(\vec{u}_n)^2 = -1, \quad u_n^0 = \sqrt{1 + \mathbf{u}_n^2}. \quad (30)$$

It is important that \vec{u}_n has only 3 independent components $\mathbf{u}_n = (u_n^1, u_n^2, u_n^3)$ and u^0 is always given in terms of them.

In the limit of infinitesimal time-lapse, the proper time distance becomes

$$ds_n = dx_n^0 \sqrt{1 - \frac{\mathbf{v}_n^2}{c^2}}. \quad (31)$$

Therefore, we obtain,

$$\frac{\mathbf{v}_n}{c} = \frac{\mathbf{u}_n}{\sqrt{1 + \mathbf{u}_n^2}} = \frac{\mathbf{u}_n}{u_n^0}, \quad \mathbf{u}_n = \frac{\frac{\mathbf{v}_n}{c}}{\sqrt{1 - \frac{\mathbf{v}_n^2}{c^2}}}. \quad (32)$$

The range of velocity is $0 \leq |\mathbf{u}_n| < \infty$ for $0 \leq |\mathbf{v}_n| < c$.

For any velocity \vec{u} , its time component

$$u^0 = \sqrt{1 + \mathbf{u}^2} \left(= \frac{1}{\sqrt{1 - \frac{\mathbf{v}^2}{c^2}}} \right) \quad (33)$$

takes the values $1 \leq u^0 < \infty$ for the above range of velocities. It governs the time dilation in the sense that

$$dx_n^0 = u_n^0 ds_n, \quad (34)$$

namely $dt_n = u_n^0 d\tau_n$; see the next subsection.⁸

⁸The time component $u^0 = \sqrt{1 + \mathbf{u}^2}$ is sometimes denoted by $\gamma(\mathbf{u})$ and is called the gamma factor.

2.5 Lorentz transformation to rest frame

When O_n at a proper time length s_n has a velocity $\vec{u}_n(s_n)$ in the world frame, the O_n 's *instantaneous rest frame* in which O_n appears at rest (at the proper time length s_n) can be obtained by the Lorentz transformation (17) with $\Lambda = L(\mathbf{u}_n(s_n))$, where

$$L(\mathbf{u}) := \begin{bmatrix} u^0 & & & \\ -\mathbf{u} & I + (u^0 - 1) \hat{\mathbf{u}}\hat{\mathbf{u}}^t & & \end{bmatrix} = \begin{bmatrix} u^0 & -u^1 & -u^2 & -u^3 \\ -u^1 & 1 + (u^0 - 1) \frac{u^1 u^1}{|\mathbf{u}|^2} & (u^0 - 1) \frac{u^1 u^2}{|\mathbf{u}|^2} & (u^0 - 1) \frac{u^1 u^3}{|\mathbf{u}|^2} \\ -u^2 & (u^0 - 1) \frac{u^2 u^1}{|\mathbf{u}|^2} & 1 + (u^0 - 1) \frac{u^2 u^2}{|\mathbf{u}|^2} & (u^0 - 1) \frac{u^2 u^3}{|\mathbf{u}|^2} \\ -u^3 & (u^0 - 1) \frac{u^3 u^1}{|\mathbf{u}|^2} & (u^0 - 1) \frac{u^3 u^2}{|\mathbf{u}|^2} & 1 + (u^0 - 1) \frac{u^3 u^3}{|\mathbf{u}|^2} \end{bmatrix}, \quad (35)$$

where u^0 is given in Eq. (33). It is straightforward to show that L obeys the defining relation of the Lorentz transformation (19) and that

$$L(\mathbf{u}) \vec{u} = \begin{bmatrix} 1 \\ \mathbf{0} \end{bmatrix}, \quad (L(\mathbf{u}))^{-1} = L(-\mathbf{u}). \quad (36)$$

Hereafter, we use an upper-case letter for quantities in a coordinate system that is an instantaneous rest frame of an object, such as

$$\vec{X} = L(\mathbf{u}_n(s_n)) \vec{x}, \quad \vec{U}_m(s_m) = L(\mathbf{u}_n(s_n)) \vec{u}_m(s_m). \quad (37)$$

By construction, O_n is at rest, $\vec{U}_n(s_n) = (1, \mathbf{0})$, at $\vec{X}_n(s_n)$ in this frame. Obviously, O_n must appear at rest for O_n itself. That is, *this \vec{X} is the coordinate system with which O_n observes the world* (at the proper time length s_n).

Furthermore, the infinitesimal time-lapse dX_n^0 in $K_n(s_n)$ becomes the same as the infinitesimal proper time distance ds_n :

$$ds_n = dX_n^0 \sqrt{1 - \left(\frac{d\mathbf{X}_n}{dX_n^0} \right)^2} = dX_n^0. \quad (38)$$

The proper time length s_n , which is Lorentz-invariantly defined, gives the time flow felt by O_n .

2.6 Covariant acceleration

Along with the covariant velocity, we define the *covariant acceleration* of O_n :

$$\vec{\alpha}_n(s_n) := \frac{d\vec{u}_n(s_n)}{ds_n}. \quad (39)$$

Note that this has a dimension of an inverse length. Taking derivative of $(\vec{u}_n)^2 = -1$ with respect to s_n , we obtain

$$(\vec{\alpha}_n(s_n), \vec{u}_n(s_n)) = 0. \quad (40)$$

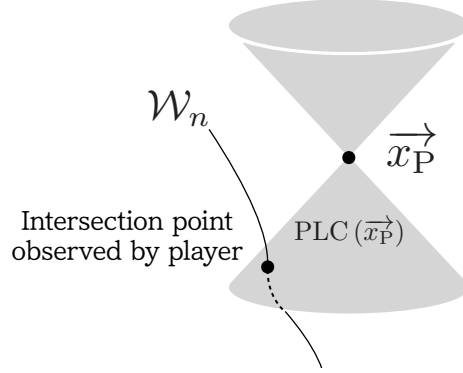


Figure 2: Schematic figure for the player's location \vec{x}_P and the intersection between $\text{PLC}(\vec{x}_P)$ and the worldline \mathcal{W}_n .

That is, the time component of the covariant acceleration is not independent of others:

$$\alpha_n^0 = \frac{\boldsymbol{\alpha}_n \cdot \mathbf{u}_n}{\sqrt{1 + \mathbf{u}_n^2}} \quad (41)$$

at any proper time length s_n in any frame. Especially, $\alpha_n^0 = 0$ whenever $\mathbf{u}_n = 0$. That is,

$$A_n^0(s_n) = 0 \quad (42)$$

in the instantaneous rest frame $K_n(s_n)$ that gives $\mathbf{U}_n(s_n) = 0$, where

$$\vec{A}_n(s_n) := L(\mathbf{u}_n(s_n)) \vec{\alpha}_n(s_n). \quad (43)$$

2.7 Past light cone

When the player P is at a spacetime point \vec{x}_P (in the world frame), the world seen by P is the collection of points from which a light ray can reach \vec{x}_P —the PLC:

$$\text{PLC}(\vec{x}_P) := \left\{ \vec{x} \mid (\vec{x} - \vec{x}_P)^2 = 0, x^0 < x_P^0 \right\}. \quad (44)$$

Note that $\text{PLC}(\vec{x}_P)$ is defined Lorentz invariantly.⁹ An object O_n is seen by the player at the intersection between its worldline \mathcal{W}_n and $\text{PLC}(\vec{x}_P)$; see Fig. 2. As said above, the player at its proper time length s_P sees the world in its instantaneous rest frame:

$$\vec{X} = L(\mathbf{u}_P(s_P)) \vec{x}. \quad (45)$$

2.8 Worldlines and their intersections with player's PLC

Here we explain how to implement the worldline in a computer game. We let the program store data of the worldlines in the world frame \vec{x} . After N iterations, O_n 's worldline \mathcal{W}_n becomes a discrete set of its past spacetime positions:

$$\mathcal{W}_n = \{ \vec{x}_{n(i)} \}_{i=0, \dots, N} = \{ \vec{x}_{n(0)}, \vec{x}_{n(1)}, \dots, \vec{x}_{n(N)} \}, \quad (46)$$

⁹The condition $x^0 < x_P^0$ is also invariant under the (orthochronous) Lorentz transformation; see footnote 1.

where we order from the past to the future.

Now we illustrate how to obtain an intersection between a particle's worldline \mathcal{W}_n and $\text{PLC}(\vec{x}_P)$. First, we check, from the past to the future, whether $\vec{x}_{n(i)} \in \mathcal{W}_n$ ($i = 0, \dots, N$) fits in the past-side of $\text{PLC}(\vec{x}_P)$:

$$(\vec{x}_{n(i)} - \vec{x}_P)^2 < 0 \quad \text{and} \quad x_{n(i)}^0 < x_P^0. \quad (47)$$

Let j ($\in \{0, \dots, N\}$) be the first iteration that violates this check. That is, $\vec{x}_{n(j-1)}$ and $\vec{x}_{n(j)}$ are the last and first spacetime points inside and outside of $\text{PLC}(\vec{x}_P)$, respectively. By linear-interpolating a point \vec{x} in between $\vec{x}_{n(j-1)}$ and $\vec{x}_{n(j)}$ as

$$\vec{x} = (1 - \lambda) \vec{x}_{n(j-1)} + \lambda \vec{x}_{n(j)}, \quad (0 \leq \lambda \leq 1), \quad (48)$$

the value of λ that gives the intersection point can be determined by the condition $(\vec{x} - \vec{x}_P)^2 = 0$:

$$\lambda = \frac{B - \sqrt{B^2 - AC}}{A}, \quad (49)$$

where

$$A := -(\vec{x}_{n(j)} - \vec{x}_{n(j-1)})^2 > 0, \quad (50)$$

$$B := -(\vec{x}_{n(j)} - \vec{x}_{n(j-1)}, \vec{x}_P - \vec{x}_{n(j-1)}) > 0, \quad (51)$$

$$C := -(\vec{x}_P - \vec{x}_{n(j-1)})^2 > 0. \quad (52)$$

We have discarded the intersection with the future light cone $(B + \sqrt{B^2 - AC})/A$.

If necessary, the O_n 's velocity on $\text{PLC}(\vec{x}_P)$, which is nothing but the velocity from $\vec{x}_{n(j-1)}$ to $\vec{x}_{n(j)}$, can be computed as

$$\vec{u}_{n(j-1)} := \frac{\vec{\Delta x}_{n(j-1)}}{\Delta s_{n(j-1)}}, \quad (53)$$

where

$$\vec{\Delta x}_{n(j-1)} := \vec{x}_{n(j)} - \vec{x}_{n(j-1)}, \quad (54)$$

$$\Delta s_{n(j-1)} := \sqrt{-\left(\vec{\Delta x}_{n(j-1)}\right)^2} = \sqrt{-(\vec{x}_{n(j)} - \vec{x}_{n(j-1)})^2}. \quad (55)$$

Accordingly, one may also store the information of the proper time length of O_n given by

$$s_{n(j)} := s_{n(j-1)} + \Delta s_{n(j-1)} \quad (56)$$

in \mathcal{W}_n .

Given $\vec{x}_{n(j)}$, $\vec{x}_{n(j-1)}$, and $\vec{x}_{n(j-2)}$, the covariant acceleration can be approximated by

$$\begin{aligned} \vec{\alpha}_{n(j-1)} &:= \frac{\vec{u}_{n(j-1)} - \vec{u}_{n(j-2)}}{\frac{\Delta s_{n(j-1)} + \Delta s_{n(j-2)}}{2}} \\ &= \frac{2}{\Delta s_{n(j-1)} + \Delta s_{n(j-2)}} \left(\frac{\vec{x}_{n(j)} - \vec{x}_{n(j-1)}}{\Delta s_{n(j-1)}} - \frac{\vec{x}_{n(j-1)} - \vec{x}_{n(j-2)}}{\Delta s_{n(j-2)}} \right). \end{aligned} \quad (57)$$

2.9 Drawing world

Once the intersecting points $\{\vec{x}_n\}_{n=1,\dots,N}$ with $\text{PLC}(\vec{x}_P)$ are obtained for N point charges, they are transformed to the player's instantaneous rest frame

$$\vec{X}_n = L(\mathbf{u}_P)(\vec{x}_n - \vec{x}_P), \quad (58)$$

where \mathbf{u}_P is the player's (dimensionless covariant) velocity at \vec{x}_P , in the world frame, and we have subtracted by \vec{x}_P to place the player at the origin of the new coordinate system.

2.10 Special relativistic equation of motion

Let m_n be the mass of O_n . In the instantaneous rest frame (37), the object O_n is at rest and hence its motion is governed by a non-relativistic equation of motion:

$$m_n c^2 \frac{d\mathbf{U}_n(s_n)}{dX_n^0} = \mathbf{F}_n(s_n), \quad (59)$$

where $\mathbf{F}_n(s_n)$ is the sum of all the non-relativistic forces felt by O_n at s_n ; recall that \mathbf{U}_n is dimensionless and that the time-length X_n^0 has the dimension of length, hence the extra factor c^2 . Since dX_n^0 here is equal to the Lorentz-*invariant* ds_n (recall Eq. (38)), we may obtain its equation of motion in the world frame by

$$m_n c^2 \frac{d\vec{u}_n(s_n)}{ds_n} = \vec{f}_n(s_n), \quad (60)$$

where

$$\vec{f}_n(s_n) := L(-\mathbf{u}_n(s_n)) \begin{bmatrix} 0 \\ \mathbf{F}_n(s_n) \end{bmatrix}, \quad (61)$$

in which we used the inverse expression (36). We stress that the time component of the equation of motion does not give independent information and can be totally neglected.¹⁰

In electromagnetism, conversely, we can directly derive \vec{f}_n in fully Lorentz-*covariant* fashion, and then derive the expression of the rest-frame force \mathbf{F}_n if necessary. The derivation of \vec{f}_n is one of the main subjects in the following.

2.11 Player's time evolution

We present a schematic time evolution for the player to account for where c appears.

In our implementation, the real-world time is synchronized with the player's proper time τ_P , or the corresponding proper time length $s_P = c\tau_P$. At the real-world time t , we have

¹⁰Indeed, Eq. (60) leads to

$$m_n c^2 \begin{bmatrix} \frac{\boldsymbol{\alpha}_n \cdot \mathbf{u}_n}{u_n^0} \\ \boldsymbol{\alpha}_n \end{bmatrix} = \begin{bmatrix} u_n^0 & \mathbf{u}_n^t \\ \mathbf{u}_n & I + (u_n^0 - 1) \hat{\mathbf{u}}_n \hat{\mathbf{u}}_n^t \end{bmatrix} \begin{bmatrix} 0 \\ \mathbf{F}_n \end{bmatrix},$$

where we used Eq. (41). The temporal and spatial components read

$$m_n c^2 \frac{\boldsymbol{\alpha}_n \cdot \mathbf{u}_n}{u_n^0} = \mathbf{u}_n \cdot \mathbf{F}_n, \quad m_n c^2 \boldsymbol{\alpha}_n = u_n^0 \mathbf{F}_{n\parallel} + \mathbf{F}_{n\perp},$$

where $\mathbf{F}_{n\parallel} := (\mathbf{F}_n \cdot \hat{\mathbf{u}}_n) \hat{\mathbf{u}}_n$ and $\mathbf{F}_{n\perp} := \mathbf{F}_n - \mathbf{F}_{n\parallel}$. Noting that $\hat{\mathbf{u}}_n \cdot \mathbf{F}_{n\perp} = 0$ and hence $\mathbf{u}_n \cdot \mathbf{F}_n = \mathbf{u}_n \cdot \mathbf{F}_{n\parallel}$, we see that the temporal component is nothing but the inner product of the spatial component with \mathbf{u}_n .

$s_P = ct$. Let Δt be the real-world time-lapse in the next iteration. Then the player's proper-time-length lapse is $\Delta s_P = c\Delta t$. In the next iteration, the player's position and velocities change into, in the world frame,¹¹

$$\vec{x}_P(s_P + \Delta s_P) = \vec{x}_P(s_P) + \vec{u}_P(s_P) \Delta s_P, \quad (62)$$

$$\mathbf{u}_P(s_P + \Delta s_P) = \mathbf{u}_P(s_P) + \boldsymbol{\alpha}_P(s_P) \Delta s_P, \quad (63)$$

where the acceleration is given as

$$\vec{\alpha}_P(s_P) = \frac{\vec{f}_P(s_P)}{m_P c^2} \quad (64)$$

from the equation of motion (60).¹²

From the dimensionalities

$$[\Delta s_P] = [c] [\text{Time}], \quad (= [\text{Length}]) \quad (65)$$

$$[\mathbf{u}_P] = [\vec{u}_P] = \left[\frac{\text{Non-relativistic velocity}}{c} \right], \quad (= [\text{Dimensionless}]) \quad (66)$$

$$[\boldsymbol{\alpha}_P] = [\vec{\alpha}_P] = \left[\frac{\text{Non-relativistic acceleration}}{c^2} \right], \quad (= \left[\frac{1}{\text{Length}} \right]) \quad (67)$$

we see that the time evolution in Eqs. (62) and (63) has the same dimensionality as the ordinary non-relativistic one.

In actual implementation, the Euler method in Eqs. (62) and (63) is known to increase the total energy of the system exponentially. Consequently, this method results in pathological behaviors such as perpetually rotating opposite charges despite the emission of electromagnetic waves. This issue can be mitigated by employing the symplectic (semi-implicit) Euler method:

$$\mathbf{u}_P(s_P + \Delta s_P) = \mathbf{u}_P(s_P) + \boldsymbol{\alpha}_P(s_P) \Delta s_P, \quad (68)$$

$$\vec{x}_P(s_P + \Delta s_P) = \vec{x}_P(s_P) + \vec{u}_P(s_P + \Delta s_P) \Delta s_P. \quad (69)$$

We utilize this symplectic Euler method in the sample code explained in Sec. 5.

2.12 Time evolution of others

At s_P , the program draws the world on $\text{PLC}(\vec{x}_P(s_P))$. In the next iteration, the program reads out the real-world time-lapse, identified as $\Delta\tau_P$, or $\Delta s_P = c\Delta\tau_P$. Then, we need to time-evolve all the point charges up to $\text{PLC}(\vec{x}_P(s_P + \Delta s_P))$. For a consistent time evolution in accordance with causality, we employ the following algorithm, which is newly explained here but has already been implemented in Ref. [2].

Let $\{ \vec{x}_n(s_n) \}_{n=1, \dots, N}$ be the last intersecting points of the N worldlines with $\text{PLC}(\vec{x}_P(s_P))$; see Fig. 2. We want to evolve the N charges consistently with causality. We first move a past-most charge with a pre-fixed small time step Δx^0 in the world frame.¹³ We then evolve the past-most one after each iteration until all the charged particles reach $\text{PLC}(\vec{x}_P(s_P + \Delta s_P))$.

¹¹The time component of the velocity can be fixed as $u_P^0(s_P + \Delta s_P) = \sqrt{1 + \mathbf{u}_P^2(s_P + \Delta s_P)}$.

¹²If the player is charged, the player will feel the electromagnetic force (93) below, which should also be added in the force in Eq. (64).

¹³In the implementation of Ref. [2], the interplay among the player and non-player characters was important. Therefore, a fixed proper-time length Δs_n was used. In the current implementation, a charge obeys only the Lorentz force and does not change its move by some extra acceleration of its own. So it suffices to consider fixed world-frame time lapse.

At each of the iterations, the position and velocity of the charge are determined by the Lorentz force described below.

3 Relativistic electromagnetism

We briefly review the relativistic electromagnetism. Once again, we ensure to include details that, although might be elementary for experts in physics and mathematics, are crucial for making the content accessible to a broader audience.

3.1 Equation of motion

In the electromagnetic dynamics, we promote the equation of motion (59) (of O_n at a space-time point \vec{x}_n with velocity \mathbf{u}_n) to¹⁴

$$m_n c^2 \frac{d\mathbf{u}_n}{dx_n^0} = \mathbf{f}_n^{\text{Lorentz}}(\vec{x}_n), \quad (70)$$

where $\mathbf{f}_n^{\text{Lorentz}}$ is the Lorentz force felt by O_n :

$$\mathbf{f}_n^{\text{Lorentz}}(\vec{x}_n) := q_n [\mathbf{E}(\vec{x}_n) + \mathbf{v}_n \times \mathbf{B}(\vec{x}_n)], \quad (71)$$

in which q_n is the charge of O_n ; \mathbf{E} and \mathbf{B} are the electric and magnetic fields at the location of the charge, respectively; \mathbf{v}_n is the non-covariant velocity (25); and the vector product is defined by, for $i = 1, 2, 3$,

$$(\mathbf{A} \times \mathbf{B})_i = \sum_{j,k=1}^3 \epsilon_{ijk} A_j B_k, \quad \begin{bmatrix} (\mathbf{A} \times \mathbf{B})_1 \\ (\mathbf{A} \times \mathbf{B})_2 \\ (\mathbf{A} \times \mathbf{B})_3 \end{bmatrix} = \begin{bmatrix} A_2 B_3 - A_3 B_2 \\ A_3 B_1 - A_1 B_3 \\ A_1 B_2 - A_2 B_1 \end{bmatrix}, \quad (72)$$

where

$$\epsilon_{ijk} = \begin{cases} 1 & \text{(when } i, j, k \text{ is an even permutation of } 1, 2, 3), \\ -1 & \text{(when } i, j, k \text{ is an odd permutation of } 1, 2, 3), \\ 0 & \text{(otherwise),} \end{cases} \quad (73)$$

is the Levi-Civita symbol, namely, the totally anti-symmetric tensor for the (spatial) rotational group $SO(3)$. With our metric covention (10), the upper and lower spatial indices are not distinguished:

$$A^i = A_i, \quad \epsilon^{ijk} = \epsilon_{ijk}, \quad (74)$$

etc.; see Eq. (87) below.

It is crucial to note that once the charge q_n is specified, the motion of O_n is governed by the electromagnetic fields. These fields are determined at any spacetime position of the charge, denoted by \vec{x}_n .

¹⁴In a more familiar-looking expression, $c \frac{d}{dx_n^0} = \frac{d}{dt}$. In the non-relativistic regime, $c\mathbf{u}_n \approx \mathbf{v}_n$, Eq. (70) reduces to the non-retivistic equation of motion $m_n \frac{d\mathbf{v}_n}{dt} \approx \mathbf{f}_n(\vec{x}_n)$. Here, we write the left-hand side of the equation of motion (70) in the form that is correct in the relativistic theory from the beginning. On the other hand, the Lorentz force (71) does not need such a modification to be relativistic.

3.2 Relativistic Maxwell's equation

Given the motion of the objects $\{O_n\}_{n=1,2,\dots}$, namely their world lines $\{\mathcal{W}_n\}_{n=1,2,\dots}$, the charge and (3D) current densities $\rho(\vec{x})$ and $\mathbf{j}(\vec{x})$ at a spacetime point \vec{x} are obtained as

$$\rho(\vec{x}) = \sum_n q_n \int ds_n \delta^4(\vec{x} - \vec{x}_n(s_n)), \quad (75)$$

$$\mathbf{j}(\vec{x}) = \sum_n q_n \int ds_n \delta^4(\vec{x} - \vec{x}_n(s_n)) c \mathbf{u}_n(s_n). \quad (76)$$

Recall that $\mathbf{u}_n(s_n)$ is dimensionless, and hence the extra factor c . Here and hereafter, we sometimes put colors for ease of eyes.

These charge and current densities determine the electromagnetic fields via Maxwell's equations at each spacetime point \vec{x} :

$$\nabla \cdot \mathbf{E}(\vec{x}) = \frac{\rho(\vec{x})}{\epsilon_0}, \quad \nabla \times \mathbf{B}(\vec{x}) = \frac{\mathbf{j}(\vec{x})}{\epsilon_0 c^2} + \frac{1}{c^2} c \partial_0 \mathbf{E}(\vec{x}), \quad (77)$$

$$\nabla \cdot \mathbf{B}(\vec{x}) = 0, \quad \nabla \times \mathbf{E}(\vec{x}) = -c \partial_0 \mathbf{B}(\vec{x}). \quad (78)$$

where, for $\mu = 0, \dots, 3$,

$$\partial_\mu := \frac{\partial}{\partial x^\mu}, \quad c \partial_0 = c \frac{\partial}{\partial x^0} = \frac{\partial}{\partial t}, \quad (79)$$

and ϵ_0 is the electric constant (vacuum permittivity).

The physical insight is most simply obtained by taking the natural units

$$\epsilon_0 = c = 1, \quad (80)$$

which also yields the natural unit for the magnetic constant (vacuum permeability) $\mu_0 := \frac{1}{\epsilon_0 c^2} = 1$. Although these constants can be easily recovered when necessary by dimensional analysis, we take the non-natural units and leave them as they are for readers unfamiliar with the dimensional analysis. Finally, even if one varies c , as in our sample program that will be described in Sec. 5, one can still safely take

$$\epsilon_0 = 1 \quad (81)$$

(yielding $\mu_0 = 1/c^2$), unless one further varies ϵ_0 .

Note that the tensor ∂_μ transforms under the inverse representation of the Lorentz group. That is, when the coordinates transforms according to Eq. (17), we obtain

$$\partial_\mu = \frac{\partial}{\partial x^\mu} \rightarrow \partial'_\nu = \frac{\partial}{\partial x'^\nu} = \sum_{\nu=1}^3 \frac{\partial x^\nu}{\partial x'^\mu} \frac{\partial}{\partial x^\nu} = \sum_{\nu=1}^3 [\Lambda^{-1}]^\nu{}_\mu \partial_\nu, \quad (82)$$

where we used

$$\frac{\partial x'^\mu}{\partial x^\nu} = \Lambda^\mu{}_\nu, \quad \frac{\partial x^\nu}{\partial x'^\mu} = [\Lambda^{-1}]^\nu{}_\mu. \quad (83)$$

We always write an inverse representation of the Lorentz group, such as ∂_μ , with the lower indices so that the contraction of all the lower and upper indices gives a Lorentz invariant.

The purely electromagnetic part (78) is automatically solved when we rewrite the magnetic and electric fields in terms of the scalar and (3D) vector potentials $\phi(\vec{x})$ and $\mathbf{A}(\vec{x})$:

$$\mathbf{B}(\vec{x}) = \nabla \times \mathbf{A}(\vec{x}), \quad \mathbf{E}(\vec{x}) = -\nabla\phi(\vec{x}) - c\partial_0\mathbf{A}(\vec{x}). \quad (84)$$

From (ϕ, \mathbf{A}) and (ρ, \mathbf{j}) , we respectively define a (covariant) vector potential \vec{A} , which we call the *gauge field* hereafter, and a (covariant) current density \vec{j} :

$$\vec{A}(\vec{x}) = (A^\mu(\vec{x}))_{\mu=0,\dots,3} := \left(\frac{\phi(\vec{x})}{c}, \mathbf{A}(\vec{x}) \right), \quad (85)$$

$$\vec{j}(\vec{x}) = (j^\mu(\vec{x}))_{\mu=0,\dots,3} := (c\rho(\vec{x}), \mathbf{j}(\vec{x})). \quad (86)$$

In the relativistic electrodynamics, we assume that they transform covariantly under the Lorentz transformation.

For any tensor such as A^μ and ∂_μ , we define

$$A_\mu := \sum_{\nu=0}^3 \eta_{\mu\nu} A^\nu, \quad \partial^\mu := \sum_{\nu=0}^3 \eta^{\mu\nu} \partial_\nu, \quad (87)$$

etc. That is, $A_0 := -A^0$, $\partial^0 := -\partial_0$ and $A_i := A^i$, $\partial^i = \partial_i$ ($i = 1, 2, 3$). Since η is the invariant tensor of the Lorentz group in the sense of Eq. (19), we see that A_μ transforms under the inverse representation of the Lorentz group, whereas ∂^μ the same as x^μ . In this notation, the inverse transformation (20), or (83), reads $[\Lambda^{-1}]^\nu{}_\mu = A_\mu{}^\nu$.

We define a rank-two anti-symmetric tensor, the *field strength*,

$$F_{\mu\nu}(\vec{x}) := \partial_\mu A_\nu(\vec{x}) - \partial_\nu A_\mu(\vec{x}). \quad (88)$$

We see that the electromagnetic fields can be written in terms of the field strength: For $i = 1, 2, 3$, Eq. (84) reads

$$\begin{aligned} E_i(\vec{x}) &= cF_{i0}(\vec{x}) = cF^{0i}(\vec{x}), \\ B_i(\vec{x}) &= \frac{1}{2} \sum_{j,k=1}^3 \epsilon_{ijk} F_{jk}(\vec{x}) = \frac{1}{2} \sum_{j,k=1}^3 \epsilon_{ijk} F^{jk}(\vec{x}). \end{aligned} \quad (89)$$

More explicitly, the magnetic reads

$$B_1(\vec{x}) = F_{23}(\vec{x}), \quad B_2(\vec{x}) = F_{31}(\vec{x}), \quad B_3(\vec{x}) = F_{12}(\vec{x}). \quad (90)$$

Now the equation of motion under the Lorentz force (70) can be written in a manifestly Lorentz-covariant (and invariant) fashion: For $\mu = 0, \dots, 3$ and for each n ,

$$m_n c \frac{du_n^\mu(s_n)}{ds_n} = q_n \sum_{\rho,\sigma=0}^3 F^{\mu\rho}(\vec{x}_n(s_n)) \eta_{\rho\sigma} u^\sigma(s_n), \quad (91)$$

or more concisely,

$$m_n c \frac{du_n^\mu(s_n)}{ds_n} = q_n \sum_{\nu=0}^3 F^{\mu\nu}(\vec{x}_n(s_n)) u_\nu(s_n), \quad (92)$$

where we have recovered the dependence on the proper time length that was implicit in Eq. (70).¹⁵

In the matrix notation (see Eqs. (143) and (144) below), the above equation of motion reads

$$m_n c \frac{d\vec{u}_n(s_n)}{ds_n} = q_n F(\vec{x}_n(s_n)) \eta \vec{u}(s_n). \quad (93)$$

This form may be more usable in practical implementation.

3.3 Relativistic Maxwell's equations

We proceed with our review of relativistic electromagnetism. Readers primarily interested in implementation aspects, rather than formalism, may choose to skip to the end of this Sec. 3.

Maxwell's equations (77) become, for $\mu = 0, \dots, 3$,

$$\sum_{\nu, \lambda=0}^3 \eta^{\nu\lambda} \partial_\nu F_{\mu\lambda}(\vec{x}) = \sum_{\sigma=0}^3 \eta_{\mu\sigma} \frac{j^\sigma(\vec{x})}{\epsilon_0 c^2}, \quad (94)$$

or more concisely,

$$\sum_{\nu=0}^3 \partial_\nu F^{\mu\nu}(\vec{x}) = \frac{j^\mu(\vec{x})}{\epsilon_0 c^2}. \quad (95)$$

In terms of the gauge field, this reads

$$\partial^\mu \left(\vec{\partial} \cdot \vec{A}(\vec{x}) \right) - \square A^\mu(\vec{x}) = \frac{j^\mu(\vec{x})}{\epsilon_0 c^2}, \quad (96)$$

where $\vec{\partial} \cdot \vec{A}(\vec{x}) := \sum_{\nu=0}^3 \partial_\nu A^\nu(\vec{x})$ and $\square := \partial^\nu \partial_\nu = -\partial_0^2 + \nabla^2$ is the d'Alembertian.¹⁶

The field strength (88) and the equation of motion (95) are *invariant* under the *gauge transformation*

$$A_\mu(\vec{x}) \rightarrow A'_\mu(\vec{x}) = A_\mu(\vec{x}) + \partial_\mu \chi(\vec{x}) \quad (97)$$

with an arbitrary real scalar function $\chi(x)$. By this degree of freedom, we can always take the gauge field to satisfy the Lorenz gauge condition:

$$\vec{\partial} \cdot \vec{A}(\vec{x}) = 0. \quad (98)$$

In the Lorenz gauge, Maxwell's equation (95) reduces to

$$-\square A^\mu(\vec{x}) = \frac{j^\mu(\vec{x})}{\epsilon_0 c^2}. \quad (99)$$

¹⁵We have used $\frac{d}{dx_n^0} = \frac{1}{u_n^0} \frac{d}{ds_n}$ in Eq. (70):

$$m_n c^2 \underbrace{\frac{du_n^i}{dx_n^0}}_{\frac{1}{u_n^0} \frac{du_n^i}{ds_n}} = q_n \left[c F^{0i} + \sum_{j,k=1}^3 \epsilon_{ijk} c \underbrace{\frac{dx_n^j}{dx_n^0}}_{c \frac{u_n^j}{u_n^0}} \left(\sum_{l,m=1}^3 \frac{1}{2} \epsilon_{klm} F_{lm} \right) \right].$$

¹⁶Here, it is understood that $\vec{\partial} = (\partial^0, \partial^1, \partial^2, \partial^3) = (-\partial_0, \partial_1, \partial_2, \partial_3)$; see Eq. (14). More explicitly, $\vec{\partial} \cdot \vec{A} = \vec{\partial}^\dagger \eta \vec{A} = \sum_{\mu=0}^3 \partial_\mu A^\mu = \partial_0 A^0 + \nabla \cdot \mathbf{A} = \frac{1}{c^2} \frac{\partial \phi}{\partial t} + \nabla \cdot \mathbf{A}$.

3.4 General solution to relativistic Maxwell's equation

Now, we review the derivation of the general solution to Eq. (99), culminating in Eq. (109) (or more concretely Eq. (107) for practical applications). As previously mentioned, readers more focused on implementation rather than formalism may opt to skip this subsection.

Using Green's function that satisfies

$$-\square G(\vec{x}) = \delta^4(\vec{x}), \quad (100)$$

the general solution to Eq. (99) can be written as

$$A^\mu(\vec{x}) = \int d^4\vec{x}' G(\vec{x} - \vec{x}') \frac{j^\mu(\vec{x}')}{\epsilon_0 c^2}, \quad (101)$$

where $\delta^4(\vec{x}) = \delta(x^0) \delta^3(\mathbf{x}) = \delta(x^0) \delta(x^1) \delta(x^2) \delta(x^3)$ is the spacetime Dirac delta function (distribution).

Now we outline the standard derivation of Green's function. By the Fourier transform

$$G(\vec{x}) = \int \frac{d^4k}{(2\pi)^4} e^{i\vec{k}\cdot\vec{x}} \tilde{G}(\vec{k}), \quad \left(= \int \frac{dk^0}{2\pi} e^{-ik^0x^0} \int \frac{d^3\mathbf{k}}{(2\pi)^3} e^{i\mathbf{k}\cdot\mathbf{x}} \tilde{G}(k^0, \mathbf{k}) \right) \quad (102)$$

$$\delta^4(\vec{x}) = \int \frac{d^4k}{(2\pi)^4} e^{i\vec{k}\cdot\vec{x}}, \quad (103)$$

we obtain

$$\tilde{G}(\vec{k}) = \frac{1}{k^2} = \frac{1}{-(k^0)^2 + \mathbf{k}^2}, \quad (104)$$

where we have adopted the notation (14). Physically, k^0 corresponds to the angular frequency $\omega = ck^0$ of the electromagnetic field, namely the light. Putting this back into the original expansion, we obtain

$$G(\vec{x}) = -\frac{1}{8\pi^2 |\mathbf{x}|} \int_0^\infty dk \left(e^{ik|\mathbf{x}|} - e^{-ik|\mathbf{x}|} \right) \int \frac{dk^0}{2\pi i} e^{-ik^0x^0} \left(\frac{1}{k^0 - k} - \frac{1}{k^0 + k} \right). \quad (105)$$

For the integration over k^0 , on physical ground, we take the retarded Green's function that takes into account only the propagation of the light from the past to the future:¹⁷

$$\begin{aligned} G_{\text{ret}}(\vec{x}) &= -\frac{1}{8\pi^2 |\mathbf{x}|} \int_0^\infty dk \left(e^{ik|\mathbf{x}|} - e^{-ik|\mathbf{x}|} \right) \underbrace{\int \frac{dk^0}{2\pi i} e^{-ik^0x^0} \left(\frac{1}{k^0 - k + i\epsilon} - \frac{1}{k^0 + k + i\epsilon} \right)}_{\theta(x^0)(-e^{-ikx^0} + e^{ikx^0})} \\ &= \frac{1}{4\pi |\mathbf{x}|} \theta(x^0) [\delta(x^0 - |\mathbf{x}|) - \delta(x^0 + |\mathbf{x}|)] = \frac{1}{4\pi |\mathbf{x}|} \delta(x^0 - |\mathbf{x}|), \end{aligned} \quad (106)$$

where ϵ is a positive infinitesimal; in the second step, we used the Fourier integral representation of the delta function $\delta(x) = \int_{-\infty}^\infty \frac{dk}{2\pi} e^{ikx}$; and in the third step, we used $|\mathbf{x}| \geq 0$.

¹⁷When $x^0 > 0$, the complex k^0 integral is closed by the contour in the lower half plane, which picks up both the positive- and negative-energy poles at $k^0 = \pm k - i\epsilon$. When $x^0 < 0$, it is closed by that in the upper half plane, which picks up no pole and the integral becomes zero.

Putting the retarded Green's function (106) into Eq. (101), we finally get the general form of the gauge field:

$$A^\mu(\vec{x}) = \frac{1}{4\pi\epsilon_0 c^2} \int d^4\vec{x}' \delta(x^0 - x'^0 - |\mathbf{x} - \mathbf{x}'|) \frac{j^\mu(\vec{x}')}{|\mathbf{x} - \mathbf{x}'|}. \quad (107)$$

Hereafter, we sometimes write the integral more concisely

$$\int_{\text{PLC}(\vec{x})} d^3\mathbf{x}' [\dots] := \int d^4\vec{x}' \delta(x^0 - x'^0 - |\mathbf{x} - \mathbf{x}'|) [\dots] \quad (108)$$

such that

$$A^\mu(\vec{x}) = \frac{1}{4\pi\epsilon_0 c^2} \int_{\text{PLC}(\vec{x})} d^3\mathbf{x}' \frac{j^\mu(\vec{x}')}{|\mathbf{x} - \mathbf{x}'|}. \quad (109)$$

Physically, \mathbf{x}' is each location of the charge in the past that affects the electromagnetic field at \vec{x} in the future. Here, the restriction of \vec{x}' onto $\text{PLC}(\vec{x})$ is achieved by imposing the time difference $x^0 - x'^0$ to be equal to the distance $|\mathbf{x} - \mathbf{x}'| \geq 0$, by the delta function.

4 Covariant formalism for field strength from point charges

We compute how the relativistic motion of a charged particle affects the electromagnetic field in the future. In other words, we compute a fully relativistic expression of the Liénard-Wiechert potential in terms of covariant quantities only. Our main goal is to find out the field strength at \vec{x} in terms of the positions and velocities of point charges on $\text{PLC}(\vec{x})$. A reader who is interested only in its final form may skip to Eqs. (141) and (142).

4.1 Continuous worldlines and covariant current density

The electromagnetic field at a spacetime point \vec{x} is determined by summing over the influence from each object O_n on $\text{PLC}(\vec{x})$, namely at the intersection between \mathcal{W}_n and $\text{PLC}(\vec{x})$. Each influence is solely determined by the position \vec{x}_n and velocity \vec{u}_n on $\text{PLC}(\vec{x})$. In the actual implementation on computers, we may always obtain them from the discrete worldline as in Sec. 2.8. Therefore, we take \vec{x}_n and \vec{u}_n for granted, and compute its electromagnetic influence on \vec{x} . This way, we treat each worldline (46) as if it were continuously parametrized by its proper time length s_n :

$$\mathcal{W}_n = \{ \vec{x}_n(s_n) \mid -\infty < s_n < \infty \}. \quad (110)$$

Given the worldlines $\{ \mathcal{W}_n \}_{n=1,2,\dots}$ of the charged particles, the covariant current density at a spacetime point \vec{x}' is given by

$$\vec{j}(\vec{x}') = \sum_n c q_n \int ds_n \delta^4(\vec{x}' - \vec{x}_n(s_n)) \vec{u}_n(s_n), \quad (111)$$

where q_n is the charge of O_n . Here, c is supplied to make the dimension of the current density (charge) / (length)² (time).

4.2 Master equation for gauge field

Here, we detail the derivation of the gauge field expression at \vec{x} in terms of the positions and velocities of point charges on PLC(\vec{x}), with its final form presented in Eq. (125).

Putting Eq. (111) into the general solution (109), or more concretely Eq. (107), the gauge field is obtained as

$$\begin{aligned} A^\mu(\vec{x}) &= \sum_n \frac{q_n}{4\pi\epsilon_0 c} \int ds_n u_n^\mu(s_n) \int d^4\vec{x}' \frac{\delta(x^0 - x'^0 - |\mathbf{x} - \mathbf{x}'|)}{|\mathbf{x} - \mathbf{x}'|} \delta^4(\vec{x}' - \vec{x}_n(s_n)) \\ &= \sum_n \frac{q_n}{4\pi\epsilon_0 c} \int ds_n u_n^\mu(s_n) \frac{\delta(x^0 - x_n^0(s_n) - |\mathbf{x} - \mathbf{x}_n(s_n)|)}{|\mathbf{x} - \mathbf{x}_n(s_n)|}. \end{aligned} \quad (112)$$

In computing this integration, we need the derivative of the argument of the delta function with respect to the proper time length. For that purpose, we define a modified gamma factor

$$\gamma_n(s_n, \mathbf{x}) := \frac{dx_n^0(s_n)}{ds_n} + \frac{\partial |\mathbf{x} - \mathbf{x}_n(s_n)|}{\partial s_n}. \quad (113)$$

To compute it, it is convenient to define the *chargeward vector* that is the covariant position vector of the charge as viewed from the reference point:

$$\vec{l}_n(s_n, \vec{x}) := \vec{x}_n(s_n) - \vec{x}, \quad \text{namely,} \quad \begin{bmatrix} l_n^0(s_n, x^0) \\ \mathbf{l}_n(s_n, \mathbf{x}) \end{bmatrix} := \begin{bmatrix} x_n^0(s_n) - x^0 \\ \mathbf{x}_n(s_n) - \mathbf{x} \end{bmatrix}. \quad (114)$$

Following the notation (9), we also write

$$\hat{\mathbf{l}}_n(s_n, \mathbf{x}) = \frac{\mathbf{l}_n(s_n, \mathbf{x})}{|\mathbf{l}_n(s_n, \mathbf{x})|}. \quad (115)$$

Now the modified gamma factor (113) can be written as

$$\gamma_n(s_n, \mathbf{x}) = u_n^0(s_n) + \hat{\mathbf{l}}_n(s_n, \mathbf{x}) \cdot \mathbf{u}_n(s_n), \quad (116)$$

where we have used the derivative (122) below.

For later use, we list derivatives with respect to \mathbf{x} ,

$$\frac{\partial l_n^i(s_n, \mathbf{x})}{\partial x^j} = -\delta^{ij}, \quad (117)$$

$$\frac{\partial |\mathbf{l}_n(s_n, \mathbf{x})|}{\partial x^i} = -\hat{l}_n^i(s_n, \mathbf{x}), \quad (118)$$

$$\frac{\partial \hat{l}_n^i(s_n, \mathbf{x})}{\partial x^j} = \frac{-\delta^{ij} + \hat{l}_n^i(s_n, \mathbf{x}) \hat{l}_n^j(s_n, \mathbf{x})}{|\mathbf{l}_n(s_n, \mathbf{x})|}, \quad (119)$$

$$\frac{\partial \gamma_n(s_n, \mathbf{x})}{\partial x^i} = \frac{-u_n^i(s_n) + \hat{l}_n^i(s_n, \mathbf{x}) \left(\hat{\mathbf{l}}_n(s_n, \mathbf{x}) \cdot \mathbf{u}_n(s_n) \right)}{|\mathbf{l}_n(s_n, \mathbf{x})|} \quad (120)$$

and derivatives with respect to s_n ,

$$\frac{\partial \mathbf{l}_n(s_n, \mathbf{x})}{\partial s_n} = \mathbf{u}_n(s_n), \quad (121)$$

$$\frac{\partial |\mathbf{l}_n(s_n, \mathbf{x})|}{\partial s_n} = \hat{\mathbf{l}}_n(s_n, \mathbf{x}) \cdot \mathbf{u}_n(s_n), \quad (122)$$

$$\frac{\partial \hat{\mathbf{l}}_n(s_n, \mathbf{x})}{\partial s_n} = \frac{\mathbf{u}_n(s_n) - \left(\hat{\mathbf{l}}_n(s_n, \mathbf{x}) \cdot \mathbf{u}_n(s_n) \right) \hat{\mathbf{l}}_n(s_n, \mathbf{x})}{|\mathbf{l}_n(s_n, \mathbf{x})|}, \quad (123)$$

$$\frac{\partial \gamma_n(s_n, \mathbf{x})}{\partial s_n} = \alpha_n^0(s_n) + \hat{\mathbf{l}}_n(s_n, \mathbf{x}) \cdot \boldsymbol{\alpha}_n(s_n) + \frac{\mathbf{u}_n^2(s_n) - \left(\hat{\mathbf{l}}_n(s_n, \mathbf{x}) \cdot \mathbf{u}_n(s_n) \right)^2}{|\mathbf{l}_n(s_n, \mathbf{x})|}. \quad (124)$$

The result of the integration (112) is, using Eqs. (113) and (114),

$$\begin{aligned} A^\mu(\vec{x}) &= \sum_n \frac{q_n}{4\pi\epsilon_0 c} \frac{u_n^\mu(s_n^*(\vec{x}))}{\left| \frac{\partial(x_n^0(s_n) + |\mathbf{x} - \mathbf{x}_n(s_n)|)}{\partial s_n} \right| |\mathbf{x} - \mathbf{x}_n(s_n)|} \\ &= \sum_n \frac{q_n}{4\pi\epsilon_0 c} \frac{u_n^\mu(s_n^*(\vec{x}))}{\gamma_n(s_n^*(\vec{x}), \mathbf{x}) |\mathbf{l}_n(s_n^*(\vec{x}), \mathbf{x})|}, \end{aligned} \quad (125)$$

where $s_n^*(\vec{x})$ is the solution to

$$x^0 - x_n^0(s_n) = |\mathbf{x} - \mathbf{x}_n(s_n)| \quad (126)$$

with respect to s_n and we have used $\gamma_n(s_n, \mathbf{x}) \geq 0$ due to $u_n^0 = \sqrt{1 + \mathbf{u}_n^2} \geq |\mathbf{u}_n|$; see Eq. (116). Physically, $s_n^*(\vec{x})$ is the proper time length that gives the intersection between $\text{PLC}(\vec{x})$ and the worldline \mathcal{W}_n . Eq. (125) is the master formula to compute the spacetime derivative of the potential $\partial_\mu A^\nu(\vec{x})$.

Technical comments

When we regard Eq. (126) as a relation among variables x^0 , \mathbf{x} , and s_n , we obtain

$$dx^0 - u_n^0(s_n) ds_n = \underbrace{\frac{\partial |\mathbf{l}_n(s_n, \mathbf{x})|}{\partial s_n}}_{\hat{\mathbf{l}}_n(s_n, \mathbf{x}) \cdot \mathbf{u}_n(s_n)} ds_n + \sum_{i=1}^3 \underbrace{\frac{\partial |\mathbf{l}_n(s_n, \mathbf{x})|}{\partial x^i}}_{-\hat{l}_n^i(s_n, \mathbf{x})} dx^i, \quad (127)$$

that is,

$$\gamma_n(s_n, \mathbf{x}) ds_n = dx^0 + \sum_{i=1}^3 \hat{l}_n^i(s_n, \mathbf{x}) dx^i. \quad (128)$$

It means

$$\frac{\partial s_n^*(\vec{x})}{\partial x^0} = \frac{1}{\gamma_n(s_n^*(\vec{x}), \mathbf{x})}, \quad \frac{\partial s_n^*(\vec{x})}{\partial x^i} = \frac{\hat{l}_n^i(s_n^*(\vec{x}), \mathbf{x})}{\gamma_n(s_n^*(\vec{x}), \mathbf{x})}. \quad (129)$$

In the master formula (125), the following equality follows from the definition of $s_n^*(\vec{x})$ being the solution to Eq. (126):

$$|\mathbf{l}_n(s_n^*(\vec{x}), \mathbf{x})| = x^0 - x_n^0(s_n^*(\vec{x})). \quad (130)$$

Using Eqs. (117)–(124) and (129), the consistency in taking the spacetime derivatives of Eq. (130) can be checked as follows: The derivative with respect to x^0 reads,

$$\left. \frac{\partial |\mathbf{l}_n(s_n^*(\vec{x}), \mathbf{x})|}{\partial x^0} \right|_{\mathbf{x} \text{ fixed}} = \left. \frac{\partial s_n^*(\vec{x})}{\partial x^0} \frac{\partial |\mathbf{l}_n(s_n, \mathbf{x})|}{\partial s_n} \right|_{s_n=s_n^*(\vec{x})} = \left. \frac{\hat{\mathbf{l}}_n(s_n, \mathbf{x}) \cdot \mathbf{u}_n(s_n)}{\gamma_n(s_n, \mathbf{x})} \right|_{s_n=s_n^*(\vec{x})}, \quad (131)$$

$$\left. \frac{\partial (x^0 - x_n^0(s_n^*(\vec{x})))}{\partial x^0} \right|_{\mathbf{x} \text{ fixed}} = 1 - \left. \frac{\partial s_n^*(\vec{x})}{\partial x^0} \frac{dx_n^0(s_n)}{ds_n} \right|_{s_n=s_n^*(\vec{x})} = \left(1 - \frac{u_n^0(s_n)}{\gamma_n(s_n, \mathbf{x})} \right) \Big|_{s_n=s_n^*(\vec{x})}. \quad (132)$$

We see that both results coincide due to Eq. (116). Similarly, the derivative with respect to x^i reads

$$\begin{aligned} \left. \frac{\partial |\mathbf{l}_n(s_n^*(\vec{x}), \mathbf{x})|}{\partial x^i} \right|_{x^0, x^j (\neq i) \text{ fixed}} &= \left. \frac{\partial s_n^*(\vec{x})}{\partial x^i} \frac{\partial |\mathbf{l}_n(s_n, \mathbf{x})|}{\partial s_n} \right|_{s_n=s_n^*(\vec{x})} + \left. \frac{\partial |\mathbf{l}_n(s_n, \mathbf{x})|}{\partial x^i} \right|_{s_n=s_n^*(\vec{x})} \\ &= \left(\left(\hat{\mathbf{l}}_n(s_n, \mathbf{x}) \cdot \mathbf{u}_n(s_n) \right) \frac{\hat{l}_n^i(s_n, \mathbf{x})}{\gamma_n(s_n, \mathbf{x})} - \hat{l}_n^i(s_n, \mathbf{x}) \right) \Big|_{s_n=s_n^*(\vec{x})}, \end{aligned} \quad (133)$$

$$\left. \frac{\partial (x^0 - x_n^0(s_n^*(\vec{x})))}{\partial x^i} \right|_{x^0, x^j (\neq i) \text{ fixed}} = - \left. \frac{\partial s_n^*(\vec{x})}{\partial x^i} \frac{dx_n^0(s_n)}{ds_n} \right|_{s_n=s_n^*(\vec{x})} = - \left. \frac{u_n^0(s_n) \hat{l}_n^i(s_n, \mathbf{x})}{\gamma_n(s_n, \mathbf{x})} \right|_{s_n=s_n^*(\vec{x})}. \quad (134)$$

We see that both results coincide again. We have verified the consistent treatment of both the time and spatial derivatives of Eq. (125) under the identity (130).

For later use, we also list the partial derivatives of the modified gamma factor restricted

onto PLC(\vec{x}):

$$\begin{aligned}
\left. \frac{\partial \gamma_n(s_n^*(\vec{x}), \mathbf{x})}{\partial x^0} \right|_{\mathbf{x} \text{ fixed}} &= \left. \frac{\partial s_n^*(\vec{x})}{\partial x^0} \frac{\partial \gamma_n(s_n, \mathbf{x})}{\partial s_n} \right|_{s_n=s_n^*(\vec{x})} \\
&= \frac{1}{\gamma_n(s_n, \mathbf{x})} \left[\alpha_n^0(s_n) + \hat{\mathbf{l}}_n(s_n, \mathbf{x}) \cdot \boldsymbol{\alpha}_n(s_n) \right. \\
&\quad \left. + \frac{\mathbf{u}_n^2(s_n) - (\hat{\mathbf{l}}_n(s_n, \mathbf{x}) \cdot \mathbf{u}_n(s_n))^2}{|\mathbf{l}_n(s_n, \mathbf{x})|} \right] \Big|_{s_n=s_n^*(\vec{x})}, \tag{135}
\end{aligned}$$

$$\begin{aligned}
\left. \frac{\partial \gamma_n(s_n^*(\vec{x}), \mathbf{x})}{\partial x^i} \right|_{x^0, x^j(\neq i) \text{ fixed}} &= \left. \frac{\partial s_n^*(\vec{x})}{\partial x^i} \frac{\partial \gamma_n(s_n, \mathbf{x})}{\partial s_n} \right|_{s_n=s_n^*(\vec{x})} + \left. \frac{\partial \gamma_n(s_n, \mathbf{x})}{\partial x^i} \right|_{s_n=s_n^*(\vec{x})} \\
&= \left\{ \frac{\hat{l}_n^i(s_n, \mathbf{x})}{\gamma_n(s_n, \mathbf{x})} \left[\alpha_n^0(s_n) + \hat{\mathbf{l}}_n(s_n, \mathbf{x}) \cdot \boldsymbol{\alpha}_n(s_n) \right. \right. \\
&\quad \left. \left. + \frac{\mathbf{u}_n^2(s_n) - (\hat{\mathbf{l}}_n(s_n, \mathbf{x}) \cdot \mathbf{u}_n(s_n))^2}{|\mathbf{l}_n(s_n, \mathbf{x})|} \right] \right. \\
&\quad \left. + \frac{-u_n^i(s_n) + \hat{l}_n^i(s_n, \mathbf{x}) (\hat{\mathbf{l}}_n(s_n, \mathbf{x}) \cdot \mathbf{u}_n(s_n))}{|\mathbf{l}_n(s_n, \mathbf{x})|} \right\} \Big|_{s_n=s_n^*(\vec{x})}. \tag{136}
\end{aligned}$$

4.3 Field strength

Using Eqs. (129), (131), and (135), we compute the time derivative of the gauge field (125):

$$\begin{aligned}
\partial_0 A^\mu(\vec{x}) &= \sum_n \frac{q_n}{4\pi\epsilon_0 c} \left[\frac{1}{\gamma_n(s_n^*(\vec{x}), \mathbf{x}) |\mathbf{l}_n(s_n^*(\vec{x}), \mathbf{x})|} \frac{\partial u_n^\mu(s_n^*(\vec{x}))}{\partial x^0} \right. \\
&\quad - \frac{u_n^\mu(s_n^*(\vec{x}))}{\gamma_n^2(s_n^*(\vec{x}), \mathbf{x}) |\mathbf{l}_n(s_n^*(\vec{x}), \mathbf{x})|} \frac{\partial \gamma_n(s_n^*(\vec{x}), \mathbf{x})}{\partial x^0} \\
&\quad \left. - \frac{u_n^\mu(s_n^*(\vec{x}))}{\gamma_n(s_n^*(\vec{x}), \mathbf{x}) |\mathbf{l}_n(s_n^*(\vec{x}), \mathbf{x})|^2} \frac{\partial |\mathbf{l}_n(s_n^*(\vec{x}), \mathbf{x})|}{\partial x^0} \right] \\
&= \sum_n \frac{q_n}{4\pi\epsilon_0 c} \left[\frac{\alpha_n^\mu(s_n)}{\gamma_n^2(s_n, \mathbf{x}) |\mathbf{l}_n(s_n, \mathbf{x})|} \right. \\
&\quad - \frac{u_n^\mu(s_n)}{\gamma_n^3(s_n, \mathbf{x}) |\mathbf{l}_n(s_n, \mathbf{x})|} \left(\alpha_n^0(s_n) + \hat{\mathbf{l}}_n(s_n, \mathbf{x}) \cdot \boldsymbol{\alpha}_n(s_n) \right. \\
&\quad \left. \left. + \frac{\mathbf{u}_n(s_n) \cdot (\mathbf{u}_n(s_n) + u_n^0(s_n) \hat{\mathbf{l}}_n(s_n, \mathbf{x}))}{|\mathbf{l}_n(s_n, \mathbf{x})|} \right) \right] \Big|_{s_n=s_n^*(\vec{x})}, \tag{137}
\end{aligned}$$

where we used $\mathbf{u}_n^2 - (\hat{\mathbf{l}}_n \cdot \mathbf{u}_n)^2 + \gamma_n (\hat{\mathbf{l}}_n \cdot \mathbf{u}_n) = \mathbf{u}_n \cdot (\mathbf{u}_n + u_n^0 \hat{\mathbf{l}}_n)$ due to Eqs. (30) and (116), in the last step.

Similarly, using Eqs. (129), (133), and (136), the spatial derivative reads

$$\begin{aligned} \partial_i A^\mu(\vec{x}) &= \sum_n \frac{q_n}{4\pi\epsilon_0 c} \left[\frac{1}{\gamma_n(s_n^*(\vec{x}), \mathbf{x}) |\mathbf{l}_n(s_n^*(\vec{x}), \mathbf{x})|} \frac{\partial u_n^\mu(s_n^*(\vec{x}))}{\partial x^i} \right. \\ &\quad - \frac{u_n^\mu(s_n^*(\vec{x}))}{\gamma_n^2(s_n^*(\vec{x}), \mathbf{x}) |\mathbf{l}_n(s_n^*(\vec{x}), \mathbf{x})|} \frac{\partial \gamma_n(s_n^*(\vec{x}), \mathbf{x})}{\partial x^i} \\ &\quad \left. - \frac{u_n^\mu(s_n^*(\vec{x}))}{\gamma_n(s_n^*(\vec{x}), \mathbf{x}) |\mathbf{l}_n(s_n^*(\vec{x}), \mathbf{x})|^2} \frac{\partial |\mathbf{l}_n(s_n^*(\vec{x}), \mathbf{x})|}{\partial x^i} \right] \\ &= \sum_n \frac{q_n}{4\pi\epsilon_0 c} \left[\frac{\hat{l}_n^i(s_n, \mathbf{x}) \alpha_n^\mu(s_n)}{\gamma_n^2(s_n, \mathbf{x}) |\mathbf{l}_n(s_n, \mathbf{x})|} + \frac{u_n^i(s_n) u_n^\mu(s_n)}{\gamma_n^2(s_n, \mathbf{x}) |\mathbf{l}_n(s_n, \mathbf{x})|^2} \right. \\ &\quad \left. - \frac{\hat{l}_n^i(s_n, \mathbf{x}) u_n^\mu(s_n)}{\gamma_n^3(s_n, \mathbf{x}) |\mathbf{l}_n(s_n, \mathbf{x})|} \left(\alpha_n^0(s_n) + \hat{\mathbf{l}}_n(s_n, \mathbf{x}) \cdot \boldsymbol{\alpha}_n(s_n) - \frac{1}{|\mathbf{l}_n(s_n, \mathbf{x})|} \right) \right] \Bigg|_{s_n=s_n^*(\vec{x})}, \end{aligned} \quad (138)$$

where we used $\mathbf{u}_n^2 - (\hat{\mathbf{l}}_n \cdot \mathbf{u}_n)^2 + \gamma_n (\hat{\mathbf{l}}_n \cdot \mathbf{u}_n) - \gamma_n u_n^0 = -1$ due to Eqs. (30) and (116), in the last step.

To summarize,

$$\partial_0 A^\mu(\vec{x}) = \sum_n \frac{q_n}{4\pi\epsilon_0 c} \left[\frac{\alpha_n^\mu}{\gamma_n^2 |\mathbf{l}_n|} - \frac{u_n^\mu}{\gamma_n^3 |\mathbf{l}_n|} \left(\alpha_n^0 + \hat{\mathbf{l}}_n \cdot \boldsymbol{\alpha}_n + \frac{\mathbf{u}_n \cdot (\mathbf{u}_n + u_n^0 \hat{\mathbf{l}}_n)}{|\mathbf{l}_n|} \right) \right], \quad (139)$$

$$\partial_i A^\mu(\vec{x}) = \sum_n \frac{q_n}{4\pi\epsilon_0 c} \left[\frac{\hat{l}_n^i \alpha_n^\mu}{\gamma_n^2 |\mathbf{l}_n|} + \frac{u_n^i u_n^\mu}{\gamma_n^2 |\mathbf{l}_n|^2} - \frac{\hat{l}_n^i u_n^\mu}{\gamma_n^3 |\mathbf{l}_n|} \left(\alpha_n^0 + \hat{\mathbf{l}}_n \cdot \boldsymbol{\alpha}_n - \frac{1}{|\mathbf{l}_n|} \right) \right]. \quad (140)$$

Here and hereafter, we omit the dependence on s_n and \vec{x} as well as the restriction on PLC(\vec{x}), namely, the condition $s_n = s_n^*(\vec{x})$ is implicitly put, unless otherwise stated. Now everything is written in terms of covariant quantities; recall Eqs (29), (39), (114) and (116).

The components of field strength $F_{i0} = -F_{0i} = F^{0i} = -F^{i0}$ and $F_{ij} = -F_{ji} = -F^{ji} = F^{ij}$ are now

$$\begin{aligned} F^{0i}(\vec{x}) &= -\partial_0 A^i(\vec{x}) - \partial_i A^0(\vec{x}) \\ &= \sum_n \frac{q_n}{4\pi\epsilon_0 c |\mathbf{l}_n|} \left[\hat{l}_n^i \frac{u_n^0 (\hat{\mathbf{l}}_n \cdot \boldsymbol{\alpha}_n - \frac{1}{|\mathbf{l}_n|}) - \alpha_n^0 (\hat{\mathbf{l}}_n \cdot \mathbf{u}_n)}{\gamma_n^3} + u_n^i \frac{\alpha_n^0 + \hat{\mathbf{l}}_n \cdot \boldsymbol{\alpha}_n - \frac{1}{|\mathbf{l}_n|}}{\gamma_n^3} - \frac{\alpha_n^i}{\gamma_n^2} \right], \end{aligned} \quad (141)$$

$$\begin{aligned} F^{ij}(\vec{x}) &= \partial_i A^j(\vec{x}) - \partial_j A^i(\vec{x}) \\ &= \sum_n \frac{q_n}{4\pi\epsilon_0 c |\mathbf{l}_n|} \left[\frac{\hat{l}_n^i \alpha_n^j - \hat{l}_n^j \alpha_n^i}{\gamma_n^2} - \frac{\hat{l}_n^i u_n^j - \hat{l}_n^j u_n^i}{\gamma_n^3} \left(\alpha_n^0 + \hat{\mathbf{l}}_n \cdot \boldsymbol{\alpha}_n - \frac{1}{|\mathbf{l}_n|} \right) \right], \end{aligned} \quad (142)$$

where we used Eq. (116) in the last step in Eq. (141). This expression for the field strength is one of our main results, which can be used directly in computer programs to obtain the Lorentz transformation of the electromagnetic fields below.

Given the field strength, the electric and magnetic fields can be derived from Eq. (89). For an actual implementation in a computer program, one may write the field strength as an anti-symmetric matrix F whose μ, ν components are given by the upper-indexed counterparts:

$$[F(\vec{x})]^{\mu, \nu} = F^{\mu\nu}(\vec{x}). \quad (143)$$

Then its Lorentz transformation law under the coordinate transformation $\vec{x} \rightarrow \vec{x}' = \Lambda \vec{x}$ is

$$F \rightarrow F' = \Lambda F \Lambda^t. \quad (144)$$

Accordingly, the Lorentz transformation for the electromagnetic fields are

$$E^i \rightarrow E'^i = cF'^{0i} = c[\Lambda F \Lambda^t]^{0,i}, \quad (145)$$

$$B^i \rightarrow B'^i = \frac{1}{2} \sum_{j,k=1}^3 \epsilon_{ijk} F'^{jk} = \frac{1}{2} \sum_{j,k=1}^3 \epsilon_{ijk} [\Lambda F \Lambda^t]^{j,k} \quad (146)$$

recall Eqs. (74) and (90).

4.4 Electromagnetic field

Readers primarily interested in implementation aspects, rather than formalism, may choose to skip to the end of this Sec. 4.

The above result is directly used in computer programs to obtain the Lorentz transformation law of the electromagnetic fields. It is not necessary to write down explicit formulae for the electromagnetic fields, which are not Lorentz covariant anyway. However, we proceed to obtain the ones manifestly written in terms of the covariant quantities only, in order to compare them with the literature.

The electromagnetic fields (89) are now

$$\begin{aligned} E^i(\vec{x}) &= cF^{0i}(\vec{x}) \\ &= \sum_n \frac{q_n}{4\pi\epsilon_0 |\mathbf{l}_n|} \left[\hat{l}_n^i \frac{u_n^0 (\hat{\mathbf{l}}_n \cdot \boldsymbol{\alpha}_n - \frac{1}{|\mathbf{l}_n|})}{\gamma_n^3} - \alpha_n^0 (\hat{\mathbf{l}}_n \cdot \mathbf{u}_n) + u_n^i \frac{\alpha_n^0 + \hat{\mathbf{l}}_n \cdot \boldsymbol{\alpha}_n - \frac{1}{|\mathbf{l}_n|}}{\gamma_n^3} - \frac{\alpha_n^i}{\gamma_n^2} \right], \end{aligned} \quad (147)$$

$$\begin{aligned} B^i(\vec{x}) &= \frac{1}{2} \sum_{j,k} \epsilon^{ijk} F^{jk}(\vec{x}) \\ &= \sum_n \frac{q_n}{4\pi\epsilon_0 c |\mathbf{l}_n|} \left\{ \hat{\mathbf{l}}_n \times \left[\frac{\boldsymbol{\alpha}_n}{\gamma_n^2} - \frac{\mathbf{u}_n}{\gamma_n^3} \left(\alpha_n^0 + \hat{\mathbf{l}}_n \cdot \boldsymbol{\alpha}_n - \frac{1}{|\mathbf{l}_n|} \right) \right] \right\}_i; \end{aligned} \quad (148)$$

see Eq. (114) for the definition of \vec{l}_n .¹⁸ From the above expression, we immediately see

$$c\mathbf{B}(\vec{x}) = -\hat{\mathbf{l}}_n(\vec{x}) \times \mathbf{E}(\vec{x}). \quad (149)$$

¹⁸More explicitly, the magnetic field is derived as

$$\begin{aligned} B_i(\vec{x}) &= \frac{1}{2} \sum_{j,k} \epsilon_{ijk} F_{jk}(\vec{x}) = \sum_n \frac{q_n}{4\pi\epsilon_0 c |\mathbf{l}_n|} \frac{1}{2} \sum_{j,k} \epsilon_{ijk} \left[\frac{\hat{l}_n^j \alpha_n^k - \hat{l}_n^k \alpha_n^j}{\gamma_n^2} - \frac{\hat{l}_n^j u_n^k - \hat{l}_n^k u_n^j}{\gamma_n^3} \left(\alpha_n^0 + \hat{\mathbf{l}}_n \cdot \boldsymbol{\alpha}_n - \frac{1}{|\mathbf{l}_n|} \right) \right] \\ &= \sum_n \frac{q_n}{4\pi\epsilon_0 c |\mathbf{l}_n|} \left[\frac{(\hat{\mathbf{l}} \times \boldsymbol{\alpha}_n)_i}{\gamma_n^2} - \frac{(\hat{\mathbf{l}}_n \times \mathbf{u}_n)_i}{\gamma_n^3} \left(\alpha_n^0 + \hat{\mathbf{l}}_n \cdot \boldsymbol{\alpha}_n - \frac{1}{|\mathbf{l}_n|} \right) \right] = (\text{last expression in Eq. (148)}). \end{aligned}$$

where we have abbreviated as $\hat{\boldsymbol{l}}_n(\vec{\boldsymbol{x}}) := \hat{\boldsymbol{l}}_n(s_n^*(\vec{\boldsymbol{x}}), \boldsymbol{x})$. Then the Poynting vector reads

$$\boldsymbol{S} := \epsilon_0 c^2 \boldsymbol{E}(\vec{\boldsymbol{x}}) \times \boldsymbol{B}(\vec{\boldsymbol{x}}) = -\epsilon_0 c \left[\boldsymbol{E}^2(\vec{\boldsymbol{x}}) \hat{\boldsymbol{l}}_n(\vec{\boldsymbol{x}}) - \left(\boldsymbol{E}(\vec{\boldsymbol{x}}) \cdot \hat{\boldsymbol{l}}_n(\vec{\boldsymbol{x}}) \right) \boldsymbol{E}(\vec{\boldsymbol{x}}) \right], \quad (150)$$

which represents the energy flux (power flow) of the electromagnetic field.

4.5 Comparison with literature

As mentioned above, readers more focused on implementation rather than formalism may opt to skip this subsection.

To compare with the expressions in the literature, it is convenient to define the non-covariant acceleration for each point charge q_n :¹⁹

$$\boldsymbol{w}_n := \frac{d^2 \boldsymbol{x}_n}{(dx_n^0)^2} = \frac{1}{c} \frac{d\boldsymbol{v}_n}{dx_n^0}, \quad (151)$$

which can be written in terms of the covariant quantities as

$$\boldsymbol{w}_n = \frac{\boldsymbol{\alpha}_n - \left(\boldsymbol{\alpha}_n \cdot \frac{\boldsymbol{u}_n}{u_n^0} \right) \frac{\boldsymbol{u}_n}{u_n^0}}{(u_n^0)^2} \left(= \frac{\boldsymbol{\alpha}_n - \alpha_n^0 \frac{\boldsymbol{u}_n}{u_n^0}}{(u_n^0)^2} \right), \quad (152)$$

where we used Eqs. (30), (32) and (34) in the first step (and Eq. (41) in the last step).

After some computation, we obtain

$$\boldsymbol{E}(\vec{\boldsymbol{x}}) = \sum_n \frac{q_n}{4\pi\epsilon_0 |\boldsymbol{l}_n| \left(1 + \frac{\hat{\boldsymbol{l}}_n \cdot \boldsymbol{u}_n}{u_n^0} \right)^3} \left[\left(\hat{\boldsymbol{l}}_n \cdot \boldsymbol{w}_n \right) \left(\hat{\boldsymbol{l}}_n + \frac{\boldsymbol{u}_n}{u_n^0} \right) - \left(1 + \frac{\hat{\boldsymbol{l}}_n \cdot \boldsymbol{u}_n}{u_n^0} \right) \boldsymbol{w}_n - \frac{\hat{\boldsymbol{l}}_n + \frac{\boldsymbol{u}_n}{u_n^0}}{|\boldsymbol{l}_n| (u_n^0)^2} \right]. \quad (153)$$

If one instead uses the *fieldward vector*,

$$\hat{\boldsymbol{n}}_n(\vec{\boldsymbol{x}}) := -\hat{\boldsymbol{l}}_n(\vec{\boldsymbol{x}}), \quad (154)$$

from the point charge to the reference point $\vec{\boldsymbol{x}}$, one may rewrite this as

$$\boldsymbol{E}(\vec{\boldsymbol{x}}) = \sum_n \frac{q_n}{4\pi\epsilon_0 |\boldsymbol{l}_n| \left(1 - \frac{\hat{\boldsymbol{n}}_n \cdot \boldsymbol{u}_n}{u_n^0} \right)^3} \left[\left(\hat{\boldsymbol{n}}_n \cdot \boldsymbol{w}_n \right) \left(\hat{\boldsymbol{n}}_n - \frac{\boldsymbol{u}_n}{u_n^0} \right) - \left(1 - \frac{\hat{\boldsymbol{n}}_n \cdot \boldsymbol{u}_n}{u_n^0} \right) \boldsymbol{w}_n + \frac{\hat{\boldsymbol{n}}_n - \frac{\boldsymbol{u}_n}{u_n^0}}{|\boldsymbol{l}_n| (u_n^0)^2} \right]. \quad (155)$$

Hereafter, we mainly use the fieldward vector $\hat{\boldsymbol{n}}_n$ to indicate direction, and the chargeward vector $|\boldsymbol{l}_n|$ to denote the distance between the field and charge.

We have explicitly checked that our result (155) coincides with the non-covariant expression in Eq. (3.29) in Chapter 9 in Ref. [4]:

$$\boldsymbol{E}(\vec{\boldsymbol{x}}) = \sum_n \frac{q_n}{4\pi\epsilon_0} \left(\frac{\left(\hat{\boldsymbol{n}}_n - \frac{\boldsymbol{v}_n}{c} \right) \left(1 - \frac{v_n^2}{c^2} \right)}{\left(1 - \hat{\boldsymbol{n}}_n \cdot \frac{\boldsymbol{v}_n}{c} \right)^3 |\boldsymbol{l}_n|^2} + \frac{\hat{\boldsymbol{n}}_n \times \left(\left(\hat{\boldsymbol{n}}_n - \frac{\boldsymbol{v}_n}{c} \right) \times \frac{1}{c} \frac{d\boldsymbol{v}_n}{dx_n^0} \right)}{\left(1 - \hat{\boldsymbol{n}}_n \cdot \frac{\boldsymbol{v}_n}{c} \right)^3 |\boldsymbol{l}_n|} \right); \quad (156)$$

¹⁹Throughout this paper, accelerations are written in units of $(\text{length})^{-1}$; see the comment after Eq. (39).

recall that $1 - \frac{v_n^2}{c^2} = 1/(u_n^0)^2$; see Eq. (34). Otherwise, in the large $|\mathbf{l}_n|$ limit, the last term in the square brackets of our result (155) drops out and, using $\mathbf{v}_n = c\mathbf{u}_n/u_n^0$, we reproduce the approximate Eq. (73.8) in Ref. [5]:²⁰

$$\mathbf{E}(\vec{x}) = \sum_n \frac{q_n}{4\pi\epsilon_0 |\mathbf{l}_n|} \frac{\hat{\mathbf{n}}_n \times [(\hat{\mathbf{n}}_n - \frac{\mathbf{v}_n}{c}) \times \mathbf{w}_n]}{(1 - \hat{\mathbf{n}}_n \cdot \frac{\mathbf{v}_n}{c})^3} + \mathcal{O}(|\mathbf{l}_n|^{-2}). \quad (157)$$

4.6 Various limits

As mentioned above, readers more focused on implementation rather than formalism may opt to skip this subsection.

Let us examine the various limits of the result. First, the non-relativistic limit $\mathbf{u}_n \rightarrow 0$ yields $u_n^0 \rightarrow 1$ and $\mathbf{w}_n \rightarrow \boldsymbol{\alpha}_{n\perp}$, where $\boldsymbol{\alpha}_{n\perp} := \boldsymbol{\alpha}_n - \hat{\mathbf{n}}_n (\hat{\mathbf{n}}_n \cdot \boldsymbol{\alpha}_n)$ is the acceleration in the direction perpendicular to the line of sight. In the limit, the contribution from the charge q_n to the electromagnetic fields, \mathbf{E}_n and \mathbf{B}_n , becomes

$$\mathbf{E}_n(\vec{x}) \rightarrow \frac{q_n}{4\pi\epsilon_0 |\mathbf{l}_n|} \left(-\boldsymbol{\alpha}_{n\perp} + \frac{\hat{\mathbf{n}}_n}{|\mathbf{l}_n|} \right), \quad (158)$$

$$\mathbf{B}_n(\vec{x}) \rightarrow \frac{q_n}{4\pi\epsilon_0 c |\mathbf{l}_n|} (-\hat{\mathbf{n}}_n \times \boldsymbol{\alpha}_{n\perp}). \quad (159)$$

In the further limit of non-acceleration $\boldsymbol{\alpha}_{n\perp} \rightarrow 0$, we recover the ordinary Coulomb's law: $\mathbf{E}_n(\vec{x}) \rightarrow \frac{q_n}{4\pi\epsilon_0} \frac{\hat{\mathbf{n}}_n}{|\mathbf{l}_n|^2}$ and $\mathbf{B}_n(\vec{x}) \rightarrow 0$.

Second, in the limit of non-acceleration, $\boldsymbol{\alpha}_n \rightarrow 0$, yielding $\alpha_n^0 \rightarrow 0$ and $\mathbf{w}_n \rightarrow 0$, the charge q_n contributes to the electromagnetic field as

$$\mathbf{E}_n(\vec{x}) \rightarrow \frac{q_n}{4\pi\epsilon_0 |\mathbf{l}_n|^2 (u_n^0 - \hat{\mathbf{n}}_n \cdot \mathbf{u}_n)^3} (u_n^0 \hat{\mathbf{n}}_n - \mathbf{u}_n), \quad (160)$$

$$\mathbf{B}_n(\vec{x}) \rightarrow \frac{q_n}{4\pi\epsilon_0 c |\mathbf{l}_n|^2 (u_n^0 - \hat{\mathbf{n}}_n \cdot \mathbf{u}_n)^3} (-\hat{\mathbf{n}}_n \times \mathbf{u}_n). \quad (161)$$

We see that further non-relativistic limit $\mathbf{u}_n \rightarrow 0$ again recovers Coulomb's law. It is also noteworthy that, at a large distance $|\mathbf{l}_n|$, the leading $|\mathbf{l}_n|^{-1}$ contribution disappears when there is no acceleration.

Third, in the ultra-relativistic limit $|\mathbf{u}_n| \gg 1$, the charge q_n contributes to the electromagnetic fields as

$$\mathbf{E}_n(\vec{x}) \rightarrow \frac{q_n}{4\pi\epsilon_0 |\mathbf{l}_n| (1 - \hat{\mathbf{n}}_n \cdot \hat{\mathbf{u}}_n)^3 |\mathbf{u}_n|^2} \left[\left(\hat{\mathbf{n}}_n \cdot \boldsymbol{\alpha}_{n\perp} + \frac{1}{|\mathbf{l}_n|} \right) (\hat{\mathbf{n}}_n - \hat{\mathbf{u}}_n) - (1 - \hat{\mathbf{n}}_n \cdot \hat{\mathbf{u}}_n) \boldsymbol{\alpha}_{n\perp} \right], \quad (162)$$

$$\mathbf{B}_n(\vec{x}) \rightarrow -\frac{q_n}{4\pi\epsilon_0 c |\mathbf{l}_n| (1 - \hat{\mathbf{n}}_n \cdot \hat{\mathbf{u}}_n)^3 |\mathbf{u}_n|^2} \left\{ \hat{\mathbf{n}}_n \times \left[\left(\hat{\mathbf{n}}_n \cdot \boldsymbol{\alpha}_{n\perp} + \frac{1}{|\mathbf{l}_n|} \right) \hat{\mathbf{u}}_n + (1 - \hat{\mathbf{n}}_n \cdot \hat{\mathbf{u}}_n) \boldsymbol{\alpha}_{n\perp} \right] \right\}, \quad (163)$$

²⁰Recall the vector calculus formula:

$$\begin{aligned} (\mathbf{A} \times (\mathbf{B} \times \mathbf{C}))_i &= \sum_{j,k} \epsilon_{ijk} A_j \left(\sum_{l,m} \epsilon_{klm} B_l C_m \right) = \sum_{j,l,m} \left(\sum_k \epsilon_{ijk} \epsilon_{lmk} \right) A_j B_l C_m \\ &= \sum_{j,l,m} (\delta_{il} \delta_{jm} - \delta_{im} \delta_{jl}) A_j B_l C_m = (\mathbf{B} (\mathbf{A} \cdot \mathbf{C}) - (\mathbf{A} \cdot \mathbf{B}) \mathbf{C})_i, \end{aligned}$$

where the last step is valid only when \mathbf{A} and \mathbf{B} are commutative as in the current consideration.

where $\boldsymbol{\alpha}_{n\perp} := \boldsymbol{\alpha}_n - (\boldsymbol{\alpha}_n \cdot \hat{\boldsymbol{u}}_n) \hat{\boldsymbol{u}}_n$ is the acceleration in the direction perpendicular to the velocity. In the further limit of the motion toward the line of sight, $\hat{\boldsymbol{u}}_n \rightarrow \hat{\boldsymbol{n}}_n$, both the denominator and numerator go to zero, and the sub-leading ultra-relativistic contributions that are omitted in Eqs. (162) and (163) will provide the results (166) and (167) below.

Finally, along the direction $\hat{\boldsymbol{n}}_n \rightarrow \hat{\boldsymbol{u}}_n$, the charge q_n contributes to the electromagnetic fields as

$$\boldsymbol{E}_n(\vec{x}) \rightarrow \frac{q_n}{4\pi\epsilon_0 |\boldsymbol{l}_n| \left(1 - \frac{|\boldsymbol{u}_n|}{u_n^0}\right)^2} \left[-\boldsymbol{w}_{n\perp} + \frac{\hat{\boldsymbol{n}}_n}{|\boldsymbol{l}_n| (u_n^0)^2} \right], \quad (164)$$

$$\boldsymbol{B}_n(\vec{x}) \rightarrow -\frac{q_n}{4\pi\epsilon_0 c |\boldsymbol{l}_n| \left(1 - \frac{|\boldsymbol{u}_n|}{u_n^0}\right)^2} \hat{\boldsymbol{n}}_n \times \boldsymbol{w}_{n\perp}. \quad (165)$$

If we further take the ultra-relativistic limit $|\boldsymbol{u}_n| \rightarrow \infty$, we obtain

$$\boldsymbol{E}_n(\vec{x}) \rightarrow \frac{4|\boldsymbol{u}_n|^2 q_n}{4\pi\epsilon_0 |\boldsymbol{l}_n|} \left(-\boldsymbol{\alpha}_{n\perp} + \frac{\hat{\boldsymbol{n}}_n}{|\boldsymbol{l}_n|} \right), \quad (166)$$

$$\boldsymbol{B}_n(\vec{x}) \rightarrow -\frac{4|\boldsymbol{u}_n|^2 q_n}{4\pi\epsilon_0 c |\boldsymbol{l}_n|} \hat{\boldsymbol{n}}_n \times \boldsymbol{\alpha}_{n\perp}, \quad (167)$$

where $\boldsymbol{\alpha}_{n\perp} \rightarrow \boldsymbol{\alpha}_{n\perp}$ due to $\hat{\boldsymbol{n}}_n \rightarrow \hat{\boldsymbol{u}}_n$.

5 Overview of concrete implementation

We have developed a sample code to demonstrate a practical implementation [6]. Below, we describe its functionality.

In our visualization of electric and magnetic fields, they are represented by green and yellow arrows, respectively. The electromagnetic fields are evaluated at lattice points, initially located on two planes perpendicular to each other, on the player's PLC. The speed of light c is expressed in units of this lattice grid as grid/s.

Positive and negative charges are represented by red and blue regular icosahedrons, respectively. We may define an arbitrary unit charge, say the elementary charge e , to be dimensionless: In the sample program, we choose to set $e/4\pi\epsilon_0 = 1$ for simplicity of the code, while retaining the dimensionality of c .²¹ In the sample program, we choose q_n to be $q_n = \pm e$ for the positive and negative charges; the values of the charges can be modified in the code if necessary.

5.1 Speed of Light

We have implemented a slider that adjusts the value of c by factors of 2^n , where the integer n ranges from -3 to 10 . When c is increased, the simulation continues unchanged, while when c is decreased, the simulation is reset to its initial configuration so that the speed of massive charges never exceed c .

²¹The fine structure constant is dimensionless and is represented as $\alpha = e^2/4\pi\epsilon_0\hbar c \simeq 1/137.$, where e is the elementary charge and $\hbar c \simeq 0.20 \text{ GeV fm}$ (in SI units, $e \simeq 1.6 \times 10^{-19} \text{ C}$ and $\hbar c \simeq 3.2 \times 10^{-26} \text{ J m}$). Therefore, in natural units $\hbar = c = \epsilon_0 = 1$, the elementary charge e becomes dimensionless and has a fixed value $e \simeq 0.30$. On the other hand, in the sample program, we take $\epsilon_0 = 1$ (see Eq. (81)) and leave c dimensional, while setting $e = 4\pi\epsilon_0 (= 4\pi)$.

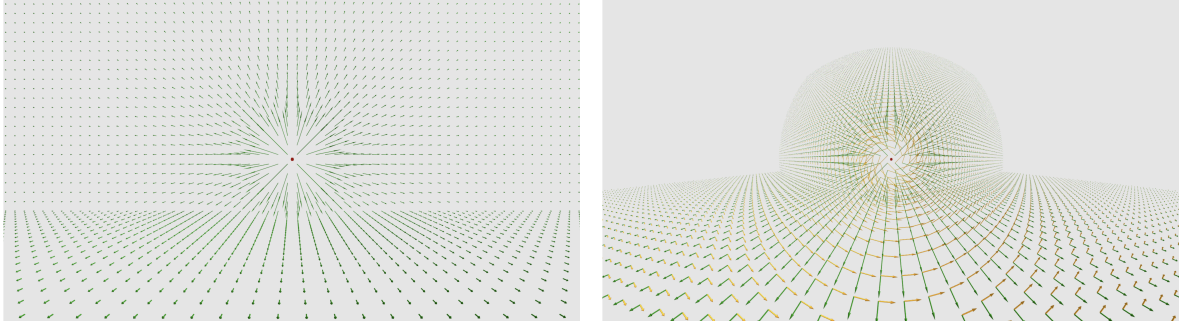


Figure 3: Scene of the sample program with the Static Charge preset. Electromagnetic fields are depicted on vertical and horizontal planes. The setup is $c = 1$ grid/s, Log Reduction Count $N = 1$, and 10-Exponent $n = 2$. **Left:** Static Coulomb electric fields (green arrows) emanate from the positive point charge at rest (red icosahedron). **Right:** After forward acceleration of the player, the point charge appears to move toward the player, generating an electric current; this produces magnetic fields (yellow arrows) circulating around the charge’s velocity vector toward the player. The planes are Lorentz contracted due to the player acceleration, actually elongated along the direction of acceleration; see Appendix B in Ref. [2] for a detailed explanation.

We have also implemented a button that allows users to disable the Lorentz transformation to the player’s rest frame (58). Note that even with the Lorentz transformation disabled, the world is still viewed from the player’s PLC.

5.2 Arrow

The length ℓ of each arrow is defined such that the electric field at a distance of 1 grid unit from the point charge is represented by an arrow with length 1 grid unit when the Log Reduction Count $N = 0$ and the 10-Exponent $n = 0$, both of which are explained below. The length of the arrows for the magnetic field is defined to match that for the electric field when $c = 1$ grid/s and when $|\mathbf{B}| = |\mathbf{E}|/c$, such as when \mathbf{E} is perpendicular to the line of sight $\hat{\mathbf{l}}$; see Eq. (149).

We also provide an option for displaying the Poynting vector (150) with magenta arrows. The length of the arrows for the Poynting vector is defined such that it becomes the same as that for the electric field when $c = 1$ grid/s and when \mathbf{E} and \mathbf{B} are perpendicular to each other, $|\mathbf{S}| = \epsilon_0 c^2 |\mathbf{B}| |\mathbf{E}|$.

Given that ℓ can vary significantly across different lattice points, we have implemented a “Log Reduction” scaling option to manage this variability. This scaling applies the transformation

$$\ell \mapsto \ln(1 + \ell) \tag{168}$$

iteratively, N times, where \ln represents the natural logarithm. We refer to N as the “Log Reduction Count.” Additionally, we implement scaling by an extra factor of 10^n before applying the Log Reduction, where n is referred to as the “10-Exponent.”

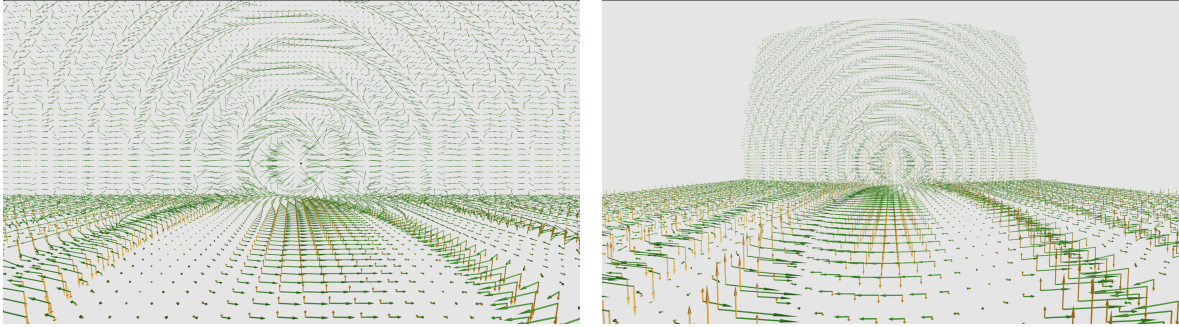


Figure 4: Scene of the sample program with the Harmonic Oscillator preset, with $c = 4$ grid/s, Log Reduction Count $N = 1$, and 10-Exponent $n = 2$; other explanations of Fig. 3 apply here too unless otherwise stated. **Left:** Electromagnetic fields (green and yellow arrows) emitted from the positive point charge (red icosahedron) under forced harmonic oscillation. The emission of electromagnetic waves is apparent both in the vertical and horizontal planes. **Right:** With the forward acceleration of the player, the planes are Lorentz contracted/elongated as in the Right of Fig. 3. On the real-time simulator, one can observe an increase in the oscillation frequency, where the time “contraction” of the incoming charge is observed; see Appendix C in Ref. [2] for a detailed explanation. In both Left and Right, the horizontal plane exhibits apparently non-spherical waves because it does not correspond to a plane on a fixed time slice of the world frame but on the player’s PLC, such that the more distant region corresponds to the further past.

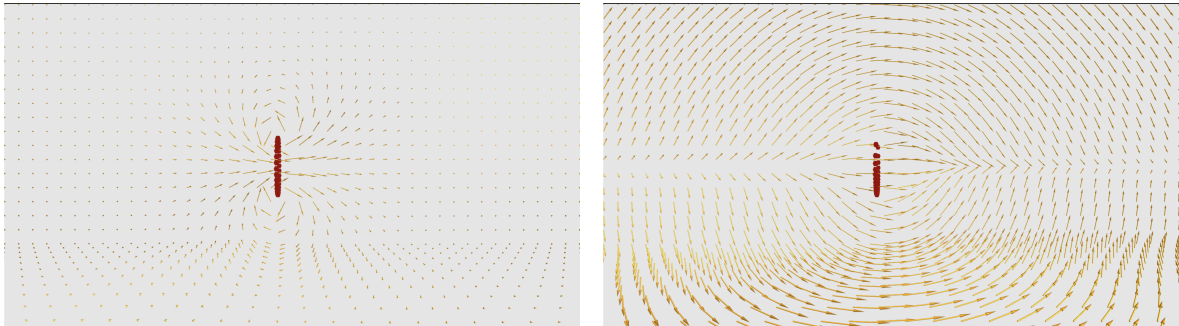


Figure 5: Scene of the sample program with the Current Loop preset, with $c = 4$ grid/s, Log Reduction Count $N = 2$, and 10-Exponent $n = 2$; other explanations from Fig. 3 apply here as well, unless otherwise stated. The electric field is not displayed here. **Left:** Magnetic field winding around the electric current generated by the rotating loop of positive charges at a non-relativistic speed. The magnetic flux through the loop appears as expected, with the direction of the flux being from left to right inside the loop and from right to left outside the loop. **Right:** At an ultra-relativistic speed of the charges, a vortex-like magnetic field is produced along the rotation axis. Both inside and outside the loop, the direction of the magnetic flux becomes from left to right. The charges on the upper (lower) side move toward (away from) the viewer, becoming sparse (dense) due to Lorentz stretching (contraction), as explained at the end of the caption for Fig. 3. In the real-time simulation, one can observe the dramatic transition from Left to Right.

5.3 Preset

Regarding the sources of electromagnetic fields, we offer multiple preset configurations:

1. Static Neg & Rotating Pos: A fixed negative charge, paired with a dynamical positive charge.
2. Dynamic Opposite Charges: A pair of positive and negative dynamical charges.
3. Static Charge: A static charge; see Fig. 3.
4. Oscillating Charge: A positive charge undergoing predetermined harmonic oscillation; see Fig. 4.
5. Current Loop: A loop of positive charges is initially at rest. Its rotation accelerates towards the speed of light.²² The electric field is not displayed in the default setup to focus on the magnetic field. At non-relativistic speeds of the charges, the magnetic field exhibits the typical winding around the current, resulting in flux from left to right inside the loop and from right to left outside it. As the rotation of the charges accelerates, one can observe a dramatic transition to a vortex-like magnetic flux, with the flux direction being from left to right both inside and outside the loop.

In the first two presets, the dynamical charges adhere to the fully relativistic equation of motion as given in Eq.(93), with their time evolution outlined in Sec. 2.12.

5.4 Grid

For visualizing electromagnetic fields, two rendering options are provided:

- Visualization only at lattice points located on two mutually perpendicular planes.
- Visualization at all lattice points within a three-dimensional grid.

5.5 Controls

On a tablet device, such as a smartphone, acceleration in the direction of sight is achieved by pinching out the screen, while pinching in results in acceleration in the opposite direction. Braking is accomplished by double-tapping the screen. The line of sight can be rotated by swiping.

When using a keyboard, constant acceleration towards the forward, backward, left, and right directions is achieved by pressing the W, S, A, and D keys, respectively. Similarly, upward and downward accelerations are controlled by the X and Z keys, respectively. Rolling is performed using the Q and E keys, while braking is achieved by pressing the R key.

²²Specifically, we set the angular velocity $\frac{d\theta}{dt} = \frac{c}{r} \frac{1 + \tanh(b(t-t_0))}{2}$, where r is the radius of the loop, t_0 shifts the initial time, and b is an arbitrary constant. The resultant angle behaves as $\theta(t) = \theta_0 + \frac{c}{2r} \left[t - t_0 + \frac{\ln \cosh(b(t-t_0))}{b} \right]$.

6 Conclusion

In this paper, we have presented a novel approach to visualizing the relativistic effects of electromagnetism through computer simulations. By implementing the full framework of special relativity, including the Lorentz transformation, light cones, and the relativistic dynamics of charged particles, we provide an intuitive and visually compelling way to grasp the core concepts of relativity and electromagnetism. The simulation allows users to experience the intermingling of electric and magnetic fields as observed from different inertial frames, offering a hands-on understanding of the profound connections between space, time, and electromagnetic phenomena.

Our approach extends existing non-relativistic simulations by incorporating a fully relativistic treatment of electromagnetism, ensuring that all interactions between particles and fields are handled in a Lorentz-covariant manner. This is crucial for accurately representing the behavior of electric and magnetic fields under relativistic conditions, where traditional, non-relativistic methods fall short.

A significant contribution of this work is the development of a manifestly covariant formalism for calculating the electromagnetic field from point charges, which is visualized in real-time as the observer's frame of reference changes. We have also introduced a novel simulation framework that allows users to observe the relativistic mixing of electric and magnetic fields, derived from the motion of charges within the player's past light cone. Additionally, our implementation of the special relativistic equation of motion within this framework enables users to explore the Lorentz force and its effects on charged particles in various inertial frames.

One of the key innovations of our work is the visualization of the observer-dependent electromagnetic field, which varies depending on the observer's motion. By observing how the electric and magnetic fields transform and interact in different reference frames, users can gain a deeper understanding of relativistic effects such as time dilation, Lorentz contraction, and the unification of electric and magnetic forces. Furthermore, our approach demonstrates the Lorentz stretching effect, often overlooked in conventional treatments, providing a more comprehensive picture of relativistic phenomena.

This paper not only lays the groundwork for future developments in the simulation of relativistic electromagnetism but also serves as a valuable educational tool. By making complex theoretical concepts accessible through interactive visualization, we aim to enhance the teaching and learning of relativity and electromagnetism in both academic and public settings.

Future work may include extending this simulation framework to incorporate general relativistic effects and refining the visual representation to further enhance user engagement and comprehension. We believe that the approach presented here opens new avenues for exploring and understanding the relativistic world, making abstract concepts more tangible and accessible to a wider audience.

Acknowledgement

The work of K.O. is in part supported by JSPS KAKENHI Grant No. 23K20855.

References

- [1] PARTICLE DATA GROUP collaboration, R. L. Workman et al., *Review of Particle Physics*, <https://pdg.lbl.gov>, *PTEP* **2022** (2022) 083C01.
- [2] D. Nakayama and K.-y. Oda, *Relativity for games*, *Progress of Theoretical and Experimental Physics* **2017** (2017) [[arXiv:1703.07063](https://arxiv.org/abs/1703.07063)].
- [3] A. Einstein, *On the electrodynamics of moving bodies*, *Annalen Phys.* **17** (1905) 891.
- [4] S. Sunakawa, *Riron Denjiki Gaku (Japanese, Theoretical Electromagnetism)*, 3rd Edition. Kinokuniya Company Ltd., 1999.
- [5] L. D. Landau and E. M. Lifschits, *The Classical Theory of Fields*, vol. Volume 2 of *Course of Theoretical Physics*. Pergamon Press, Oxford, 1975.
- [6] D. Nakayama, K.-y. Oda and K. Yasuda, “Sogebu Special Relativity.” <https://sogebu.github.io/special-relativity-web/20240810/>, 2024.